Cell Reports
Physical Science

CellPress
OPEN ACCESS

Review

Beyond water: Physical and heat transfer properties of phase change slurries for thermal energy storage

Alekos Ioannis Garivalis,[1,*] Damiano Rossi,[2,*] Maurizia Seggiani,[2] and Daniele Testi[1]

SUMMARY

Thermal energy storage is a key technology for decarbonization. In this context, phase change slurries (PCSs) retain the heat storage advantages of phase change materials (PCMs) while relying on fluidity to overcome heat transfer inefficiencies caused by the poor thermal conductivity of bulk PCMs. PCSs can replace water in conventional low-temperature storage tanks, offering numerous advantages. Despite their potential, there is a lack of research in this area, especially regarding natural convection heat transfer. Furthermore, addressing the complex thermo-physical and rheological properties of slurries is essential. This review focuses on the characterization, measurement, and modeling of physical properties of micro/nano-PCSs and their heat transfer performance under natural convection. The state-of-the-art in the field is presented, research gaps are identified, and directions for future research are proposed. Filling the above gaps will support the choice of PCSs as future and sound enhanced fluids for low-temperature heat storage.

INTRODUCTION

Energy demand increased abruptly from the 1950s with the growing population and the advancement of society.[1] Fossil fuels were mostly used to sustain development, leading to a concerning environment pollution and climate change due to greenhouse gas emissions. One of the most urgent challenges of the last decades is to manage the ecological transition toward a sustainable model in which energy is largely produced from renewable and clean sources and emissions are limited to environmentally sustainable levels. One of the larger parts of the global energy consumption is dedicated to heating and cooling purposes in buildings.[2] Long-term load peaks are particularly experienced during cold and hot seasons, while short-term load peaks occur on a typical daily basis. Renewable sources (e.g., solar, wind, tidal) allow for the generation of energy with minimal environmental impact; however, they are subjected to arbitrary power generation cycles, and their peak production times do not necessarily align with peak demand. In this context, energy storage becomes a key technology to realize a carbon neutral energy system.[3] Specifically, thermal energy storage (TES) can assist in balancing energy demand and supply by accumulating a significant amount of thermal energy during off-peak times. This stored energy can then be released during the peak demand periods, potentially reducing the capacity requirements of thermal generators. Furthermore, if heating and cooling are provided by heat pumps, TES can also contribute to easing the load on the electric grid.[4]

TES systems are categorized into sensible TES, in which the energy storage is associated with a variation in the temperature of the storage material; latent TES, where a

[1]Department of Energy, Systems, Territory and Constructions Engineering, University of Pisa, Largo Lucio Lazzarino 1, 56122 Pisa, Italy

[2]Department of Civil and Industrial Engineering, University of Pisa, Largo Lucio Lazzarino 1, 56122 Pisa, Italy

*Correspondence:
alekos.garivalis@unipi.it (A.I.G.),
damiano.rossi@unipi.it (D.R.)

https://doi.org/10.1016/j.xcrp.2024.101905

phase change process is included in the process; and thermo-chemical TES, in which a reversible chemical reaction allows for the storage and release of thermal energy. Sensible TES is the most studied and widespread for both low- and high-temperature applications, due to its relatively low cost and simplicity. However, its specific energy capacity is limited, and the change in temperature associated with the charge process results in an increase of thermal losses, restricting the storage period to a few hours. Thermo-chemical TES relies on storing energy in chemical bonds and transfer heat during reversible reactions. Moreover, it is stored at ambient temperature, minimizing heat losses and enabling an extended storage duration. However, its application is constrained by its high complexity and costs, with only few prototypes having been realized.[5]

Latent TES is a valuable option for increasing the specific energy storage capacity and performance as the latent heat associated with the phase change process at a constant temperature range is added. The energy storage material that changes phase is called phase change material (PCM). In principle, several transformations could be used, such as solid-solid, solid-liquid, solid-gas, and liquid-gas; however, despite solid-gas and liquid-gas being characterized by high latent heats, only the solid-liquid transformation is commonly employed due to large heat storage density and small volume change during phase change.[6]

Despite the desirable properties, PCMs often suffer from low thermal conductivity, compatibility problems with other materials, shape stability, and leakage. One way to improve PCM properties is to mix them with other materials to create composites. Usually, graphite and metal particles can be included in the PCM, or the PCM can be embedded into graphite, metal or polymeric foam or porous structures.[7]

In the last two decades, among other techniques, it has been proposed to disperse small particles of PCM in a carrier single-phase fluid, to enhance the specific energy stored as well as heat transfer. Inaba[8] named them "functionally thermal fluids" but they are commonly referred to as phase change slurries (PCSs). PCSs can serve as both heat transfer fluids and energy storage media, avoiding in this way the implementation of a secondary heat transfer fluid. Maintaining the fluidity of the storage medium, they could solve some of the common problems of the bulk PCMs, such as high thermal resistances, leaking, stability, and relatively large volume variations. Indeed, the storage medium (slurry) remains in the liquid phase even if the PCM undergoes a phase transition; thus, it could rely on convective heat transfer. PCSs experience a volume variation during the phase change, but it is usually smaller than bulk PCM, resulting in a more efficient use of the storage volume and a consequent increase of specific energy of the whole storage system. Several authors have shown that PCSs can improve heat transfer performance in terms of compactness of the storage,[9] lead to pipeline downsizing if used as a heat transfer fluid,[10] and maintain an acceptable heat transfer rate with respect to bulk storage solutions.[9]

One crucial aspect in quantifying the effectiveness of thermal storage is the charge/discharge times, which, in turn, depend on the efficiency of heat transfer. According to the literature review of PCSs, most of the attention has been devoted to the forced convection heat transfer. On the other side, despite the necessity for a comprehensive understanding of heat transfer under natural (or free) convection to fully leverage the potential of PCMs, only a limited amount of research has been conducted in this area. Indeed, in spite of its lower heat transfer rates compared with mixed and forced convection, natural convection is widely employed in many contexts, including TES for buildings, electronic cooling,[11] heat exchangers, solar collectors,

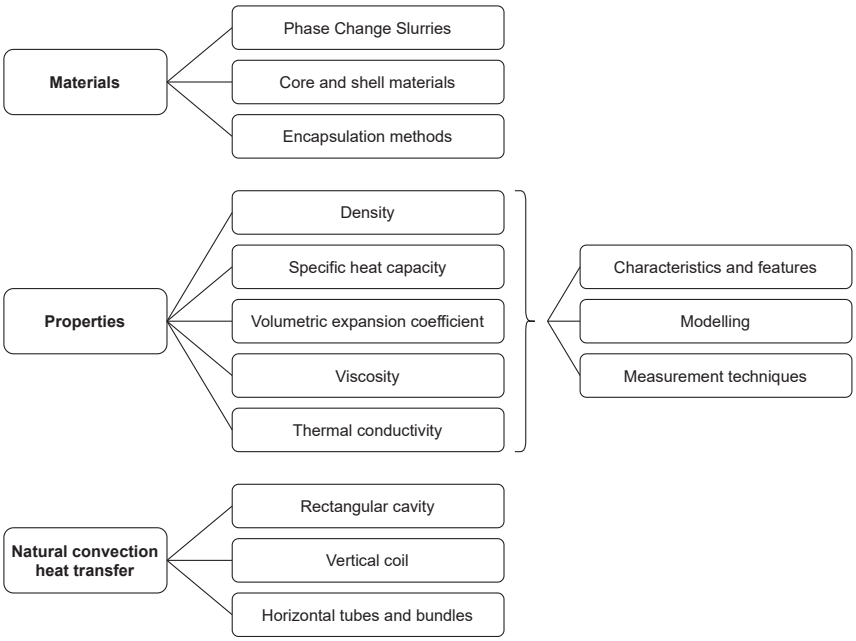

Figure 1. Schematic diagram of the review structure

and energy waste heat recovery.[12] Natural convection does not require active transfer component devices such as pumps and stirrers, thus it has advantages in terms of maintenance, cost, noise, reliability, and safety. Furthermore, the thermo-physical properties of the slurries must be considered with care, as they are more complex than those of a single-phase fluid and strictly related to the heat transfer rates. The performance of the storage is further influenced by some peculiarities of the slurries, such as hysteresis and stability.

In conclusion, while there is a considerable number of works in the literature on the forced convection heat transfer of PCSs, there is a lack of information on the natural convection. The present review primarily focuses on natural convection heat transfer in PCSs for low-temperature TES (i.e., $T < 100^{\circ}C$). This includes heating, ventilation, and air conditioning (HVAC) technologies typically employed in the construction and building sector.

This article emerges as a dedicated review dealing with natural convention in PCSs. It follows the structure presented in the schematic diagram of Figure 1. In the first section, a summary of the several PCSs developed and employed so far is presented. In the second section, the models and measurement techniques of the complex thermo-physical and transport properties of PCSs are examined, together with their most common limitations (stability, subcooling, hysteresis). Whenever possible, the proposed models describing the physical properties are compared and critically discussed, along with providing insights into the measurement methods. This comprehensive review covers all the thermo-physical properties, including the volumetric expansion coefficient, which has often been overlooked in other surveys but holds great significance in natural convection. Special attention is also given to viscosity. Then, the third section reports and critically analyses the existing studies on natural convection with PCSs in different geometries. The review ends by suggesting and discussing future research directions for PCS applications, aiming to provide valuable insights for the design of future enhanced thermal storages.

PCMs AND SLURRIES

Definition of a PCS

A PCS or latent functional thermal fluid is a mixture of at least two elements: the suspended PCM particles and the carrier fluid. When needed, some additives can be added for specific purposes. Based on the first classification of PCSs proposed by Inaba[8] and currently accepted in the literature,[9,13,14] PCSs are divided into five groups.

(1) Ice slurry: mixture of ice crystals, water, and an additive that lowers the water freezing point, limits the ice particle size, and avoids agglomeration. The PCM and the carrier fluid share the same chemical composition and exchange mass between them. A review on the topic is given by Kauffeld and Gund.[15]
(2) Phase change emulsion (PCE): a mixture of PCM particles (hydrophobic), water, and a surfactant to allow dispersion of the two insoluble components. In chemistry, an "emulsion" is composed of two liquid phases, one of which is suspended within the other. In the PCSs context, the PCM particles can be in both in solid and liquid phase according to the temperature. In PCEs, only the surfactant interposes between the PCM and the carrier fluid.
(3) Encapsulated PCS (EPCS): a mixture of PCM particles encapsulated in a shell (often a polymeric capsule) and a carrier fluid. Additives are not strictly necessary but can be used to avoid agglomeration. EPCSs are classified by particle size: capsules larger than 1,000 μm constitute macro-EPCSs; for capsules size ranging from 1 to 1,000 μm they are named micro-encapsulated slurries (MPCSs); and nano-encapsulated slurries (NPCSs) consist of capsules below 1 μm. Macro-capsules are not as advantageous compared with micro-capsules and nano-capsules as their large dimensions prevent a stable mixing with the carrier fluid, make the shell fragile, and show a large difference in temperature between the PCM core and the boundaries. This leads to suboptimal heat transfer through the capsule.[16]
(4) Clathrate hydrate slurry: crystals of clathrate hydrate suspended in aqueous solution. Clathrates are chemical compounds consisting of a lattice structure that contains molecules of another substance. Clathrate hydrates are made of water lattice trapping molecules of other substances (e.g., salts). The energy stored in the molecular structure is associated with the formation and dissociation of the clathrate.[17]
(5) Shape stabilized slurry: mixture of PCMs infiltrated in a polyethylene structure and water. Polyethylene melting temperature is higher than that of the PCMs, thus it can be confined within the structure avoiding leakage.

Among the above slurry types, the PCE and MPCM/NPCM result to be the most promising for low-temperature TES applications due to the wide range of phase change temperature, availability, and effectiveness.[6,18] In the following sections, only these PCS will be considered. Indeed, over the past two decades, several studies and reviews focused on the production, thermal and rheological properties, heat transfer capabilities, and storage applications of these slurries. Before examining their physical and heat transfer characteristics, the next sections describe the core and shell materials and the production processes of PCM particles.

Core materials of PCS particles

Cores of PCS particles are composed of pure or a mixture of PCMs, and may include some stabilizers, diluents, and other additives.[19] PCMs are usually classified according to their chemical nature into organics and inorganics. Eutectics are a special

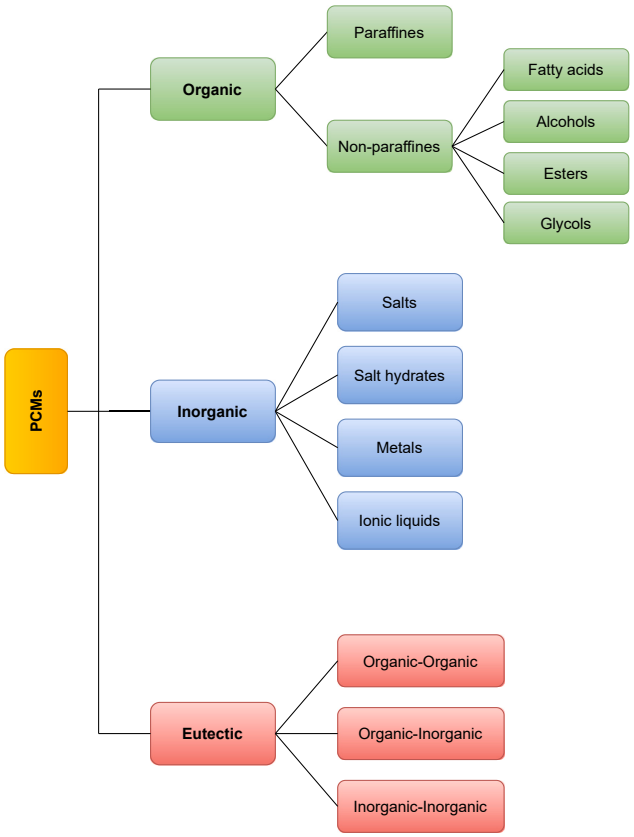

Figure 2. Classification of most common PCMs by chemical composition

group consisting of a compound of organics and/or inorganics at a specific weight ratio. Figure 2 shows the most common PCMs classified by their chemical nature. Only the solid-liquid phase change has been considered.

Organic

Organic PCMs are divided into paraffins and non-paraffins (fatty acids, alcohols, esters, etc.). They are commercially available and cheap, non-corrosive, show low degrees of subcooling, and chemical and thermal stability.[20] Moreover, their phase change temperature range can be adjusted in a large span (up to 100°C). On the other hand, they have lower latent heat (150–250 kJ/kg) compared with inorganics, are flammable, and have low thermal conductivity (around 0.2–0.3 W/mK).[21]

Paraffins are a mixture of alkanes that consist of saturated straight-chain or branched-chain hydrocarbons. They are a product of petroleum refinery, and their melting temperature varies from −57°C (octane, C_8H_{18}) to 105°C (heptacontane, C_{70}H142). Due to their properties, their wide melting temperature ranges, and availability, paraffins are the most studied PCMs; according to a recent literature survey conducted by Lawag and Ali,[21] the most studied PCMs are organic (81%) and, among them, the 79% are paraffins.

Fatty acid characteristics are similar to those of paraffins. Furthermore, they are obtained from vegetal or animal sources. They can be mixed to obtain compounds with different phase change temperatures. A detailed study on the properties of fatty acids and their potential use as PCMs for TES is by Suppes et al.[22]

Inorganic

Inorganic PCMs are salts, salt hydrates, and metals. They have higher latent heat than organics, but drawbacks such as phase segregation, subcooling, corrosion, and chemical instability. Water is considered one of the best available PCMs[7] due to its good solid-liquid phase change enthalpy (333 kJ/kg) but its application is limited by the phase change temperature (0°C and some degrees below zero, considering water-salt eutectics).

Salts are generally used for high-temperature energy storage, but they can store less specific energy than salt hydrates. Recently, ionic liquids have been proposed as PCMs, as they show low volatility and flammability and thermal and chemical stability; moreover, their high densities (1,000–1,850 kg/m^3) allow high volumetric energy storage.[23]

Salt hydrates include water molecules in their crystal structure, resulting in a substantial volumetric density of up to 350 MJ/m^3. They exhibit higher thermal conductivity than organic PCMs (about 0.5 W/mK) and are usually more cost-effective.[24] However, drawbacks include the loss of water content when heated, corrosiveness toward metal containers,[25] high degrees of subcooling, and precipitation in water due to density difference.[20]

Low-melting-point metals (gallium, indium, zinc, and their alloys) have high stored energy density and high thermal conductivity (up to 100 W/mK), overcoming some of the issues of other inorganic and organic materials.[26]

Eutectic

Eutectic refers to a mixture of chemical compounds or elements at a specific proportion characterized by a melting point lower than that of its constituents. Combinations can be organic-organic, inorganic-inorganic, and organic-inorganic.[19] Typically, the eutectic exhibits higher latent heat and lower melting point compared with the individual components.[21]

PCM characteristics and applications

In Figure 3 the melting temperature and specific enthalpy ranges for various classes of PCMs are shown. Most of them have a favorable enthalpy level; however, their applicability depends mainly on their phase change temperature. PCMs can be roughly classified according to their application into low, medium, and high temperature.[27]

Organic PCMs, such as paraffins, fatty acids, and PEGs (polyethylene glycols), have phase change temperatures aligning closely with suitable temperatures in civil engineering applications (space heating and cooling storage, HVAC systems, thermal energy management, wallboards, and ceiling tiles). Paraffins and fatty acids are the most commonly used organic PCMs, while the applications of alcohols and glycols are marginal.[30] In particular, paraffins stand out due to their broad range of melting points obtainable by their diverse mix of compounds. Fatty acids, on the other hand, present a narrower melting point range compared with petroleum-based paraffins. However, they are particularly attractive due to their improved sustainability.

In contrast, the higher phase change temperature of most inorganic PCM makes them more suitable for applications such as concentrated solar power plants,[31] Carnot batteries,[32] and industrial waste heat recovery.[12] A special class of PCMs is represented by salt-hydrates, which retain high enthalpy with a melting temperature comparable with that of organic PCMs. This latter class is also employed in

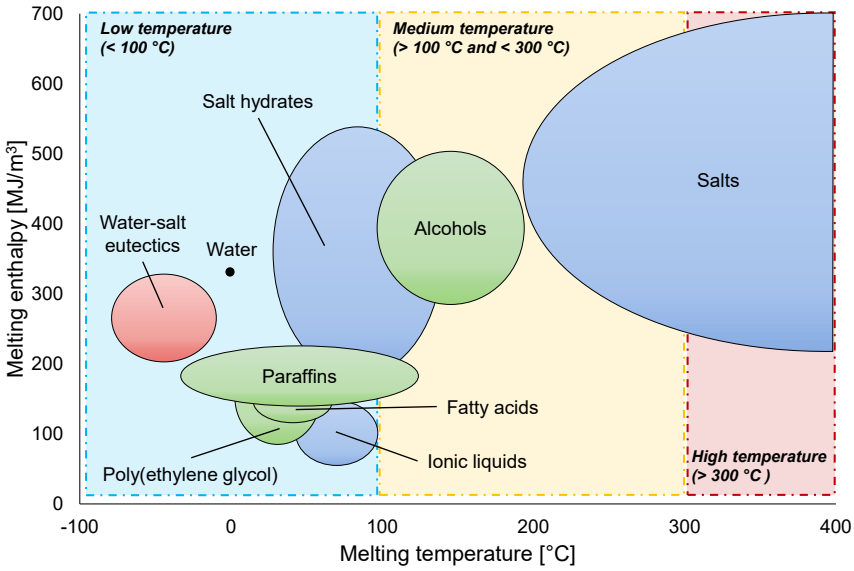

Figure 3. Schematic of PCM melting temperature and volume-specific enthalpy ranges
According to Zhu et al.[28] and Bruno et al.[29]. The colored boxes indicate a classification based on the application temperature.

low-temperature applications such as building energy conservation, solar water heat recovery, and textiles.[33]

Issues related to the flammability of organic PCMs and corrosion of inorganic ones must be considered when designing the final application. Nevertheless, incorporating PCMs into aqueous slurries could be beneficial in reducing the risk of flammability. Moreover, encapsulating the PCM core with proper and stable materials mitigates the corrosion phenomena. On the other hand, reducing the dimension of the PCM bulk by making small particles increases subcooling, thereby causing hysteresis. Further details on subcooling are given in the next section.

A detailed description of the various PCM applications according to their thermophysical properties is provided by Wang et al.[34] and Diaconu et al.[30]

Shell materials

The operational temperature of the PCM affects the choice of shell material. Polymeric shells for micro/nano-encapsulation are implemented in low- to medium-temperature applications. There are more than 50 polymers that can be used. These can be grouped into melamine, formaldehyde, and acrylic resins.[19] The shell must form a thin, strong, flexible, and stable layer surrounding the core material. Besides, it must be compatible with the core, impermeable, soluble in the carrier fluid, and, ultimately, inexpensive.

Among the group of acrylic resins, the copolymers of methacrylate are the most popular commercially employed shell materials due to their optimal mechanical and thermal properties, chemical compatibility, and easy preparation methods. Specifically, poly(methyl methacrylate) (PMMA) has gained extensive use owing to its notable thermal stability[19] and compatibility with both paraffins and fatty acids.[35] Melamine-formaldehyde resin is the other commercially available polymer that is often used as the shell.[36] Additives such as graphene oxides can be incorporated into the previous resins to further improve thermal conductivity, surface smoothness, and encapsulation efficiency.[37]

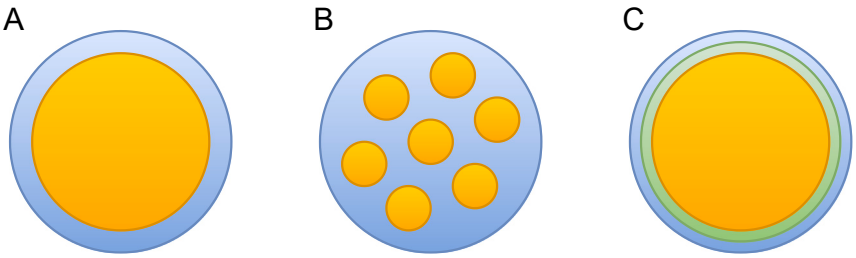

Figure 4. Common encapsulation morphologies
(A) Mono-nuclear, (B) multi-nuclear, and (C) multi-film micro-capsules.

The use of micro-capsules with polymeric shells is limited in applications where low flammability, high thermal conductivity, and high rigidity are required. In these scenarios, inorganic shells including silica (SiO_2), zinc oxide (ZnO), titanium dioxide (TiO_2), and calcium carbonate ($CaCO_3$) have been gradually employed due to their increased rigidity, superior mechanical strength, and enhanced thermal conductivity and stability.[38]

Micro/nano-encapsulation methods

The micro-encapsulation techniques were firstly employed in pharmaceutical and chemical engineering applications, and more recently considered also in heat storage and transfer applications, including buildings.[39,40]

Various morphologies can be obtained by micro-encapsulation. In PCM applications the most common types are the mono-nuclear, multi-nuclear, and multi-film capsules (Figure 4).

PCM encapsulation methods are classified according to the main mechanism of particle formation into physical, physical-chemical, and chemical processes. Each method is tailored to the specific characteristics of the material and application area, as reported in Figure 5.

Physical methods are more environmentally friendly as they do not involve chemical reactions or organic solvents. However, they are not capable of producing capsules below 50 μm[14,41]; hence, nano-capsules cannot be formed using these techniques. In vacuum impregnation technology, both organic and inorganic PCMs are incorporated into a porous matrix, such as expanded graphite or porous silica. This method enhances the thermal conductivity of the PCM due to the improved surface area between the PCM and the matrix. Spray drying and spray cooling are effective micro-encapsulation techniques, particularly suitable for preserving heat-sensitive materials. They have great potential when applied at an industrial scale, with advantages such as reduced production costs, minimized loss of raw materials and process waste, ease of control, and the ability to scale up to a large and continuous process.

Chemical methods are the encapsulation techniques that show the best performance and are primarily used in the production of commercial PCM products. They involve one or more chemical reactions and can produce micro- and nano-capsules. Typically, chemical methods are applied with organic materials as core, such as waxes and paraffins. Emulsion polymerization is a process that involves the creation of polymer composites by incorporating PCM particles into a polymer matrix, typically PMMA, polystyrene, and poly(styrene-co-ethyl acrylate), through

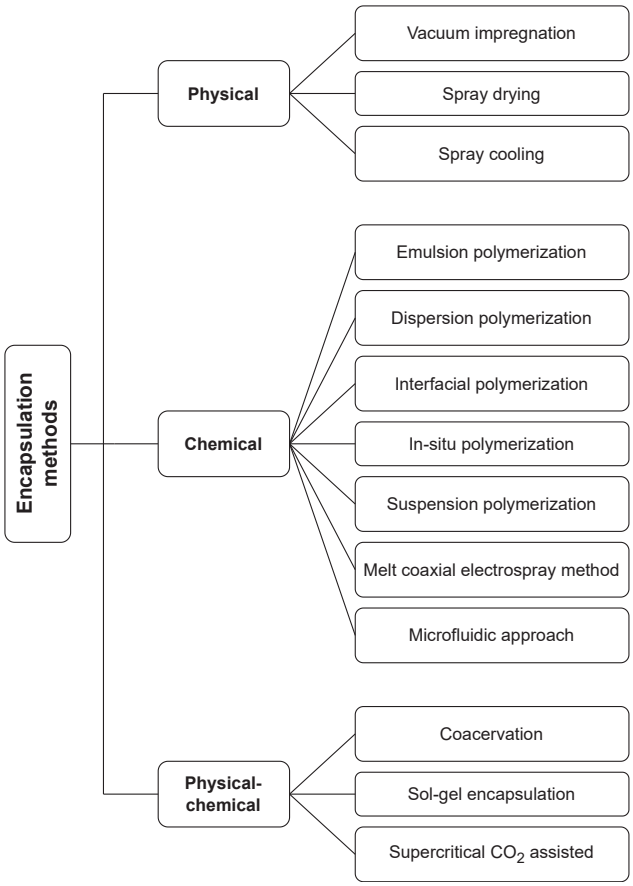

Figure 5. Overview of encapsulation methods by the main mechanism of particle formation

emulsification and subsequent polymerization. This method employs an emulsion, where PCM particles are dispersed as droplets within a continuous polymerization medium. Dispersion polymerization is another technique that integrates finely dispersed PCM particles into a developing polymer matrix during the polymerization reaction, resulting in a composite material. This method enables precise control over the size and distribution of PCM particles within the polymer structure, offering a versatile solution with tailored thermal properties suitable for applications in energy storage and temperature management. In interfacial polymerization methods, the shell is generated through the reaction between a water-soluble monomer and an organic-soluble monomer at the interface between oil and water. In the process of *in situ* polymerization, the prepolymer (typically melamine-formaldehyde or urea-formaldehyde) undergoes crosslinking at the oil-water droplets interface. This results in the formation of a continuous shell that envelops the PCM droplets. Suspension polymerization, involves a heterogeneous radical polymerization process employed in the production of various common commercial resins, including PVC, polystyrene, and PMMA. Melt coaxial electrospray and microfluidic methods are not yet widely adopted in the industry. Recently, microfluidic approaches have been proposed as an emerging technique to produce highly monodisperse PCMs with better control of properties. Despite significant advancements in both theory and technology of microfluidic techniques for PCM production, challenges related to their low throughput continue to impede their widespread adoption and commercialization.

Table 1. Manufacturers of microencapsulated PCM (to 2024)

Trademark name	PCM	Shell material	Particle size (μm)	Melting points (°C)
MikroCaps d.o.o. (Slovenia)	paraffin wax	melamine-formaldehyde/ polyurethane based	1–10	−20–70
Microtek laboratories, inc. (US)	paraffin wax	melamine and acrylic based polymers	15–30	6–19
Encapsys, LLC (US)	organic	polymer	10–50	4–45
Insilico Co. Ltd. (Republic of Korea)	paraffin wax	melamine	15	18–70

Physical-chemical methods combine physical processes (drying, heating, cooling, phase separation) with chemical processes (hydrolysis, crosslinking, polycondensation). These versatile methods are applicable to both nano- and micro-capsules. Specifically, coacervation involves the use of oppositely charged polyelectrolytes, typically gelatin as the polycation and arabic gum as the polyanion in an aqueous solution. In this process, oil phase droplets are emulsified in an aqueous phase containing gelatin. The polyanion solution is introduced to the emulsion, leading to phase separation as the pH is reduced with acid. This results in the formation of a polymer-rich phase (coacervate or PCM core) that adheres to the oil-interface droplets, creating a gelatinous shell upon cooling. Subsequent crosslinking of the shell with glutaraldehyde imparts rigidity, preventing the gelatin from melting during PCM phase transitions. Sol-gel encapsulation is a versatile method involving the transformation of a colloidal suspension (sol) into a three-dimensional gel network. This process starts with the hydrolysis of precursor molecules in the sol, leading to polymerization and gelation. The technique for encapsulating core material using supercritical fluid, such as CO_2, relies on the rapid expansion of highly compressed gases. The supercritical fluid, carrying both the core and shell material under high pressure, is discharged through a nozzle into atmospheric pressure, inducing a sudden pressure change. This pressure reduction leads to the dissolution and deposition of the shell material around the core material, ultimately forming the coating layer.

Comprehensive reviews of the encapsulation techniques (mentioning obtainable capsule size and properties) are given by Ghasemi et al.[41] and Liu et al.[42] Other details can be found in other works.[9,10,14,19,43,44]

To date, micro-EPCMs are available on the market. In Table 1, some manufacturers of MPCMs for low-temperature applications along with some characteristics of the provided PCM particles and their range of melting points are listed.

As a representative example in Figure 6, an SEM picture of some micro-capsules provided by Encapsys LLC (EnFinit PCM 28PCS) is shown together with the distribution of the particle diameters.

PROPERTIES OF MICRO- AND NANO-PCSs

PCSs can be considered as enhanced fluids with high energy storage capabilities within the phase change temperature range. Because of their biphasic nature (liquid carrier fluid with dispersed solid-liquid particles), the properties can be characterized by non-linearities and hysteresis that influence the heat transfer processes and increase the complexity of mathematical modeling.

To date, several reviews[9,14,19,44] have been published describing the thermal and physical properties of the PCSs. In this section, the methods to calculate and

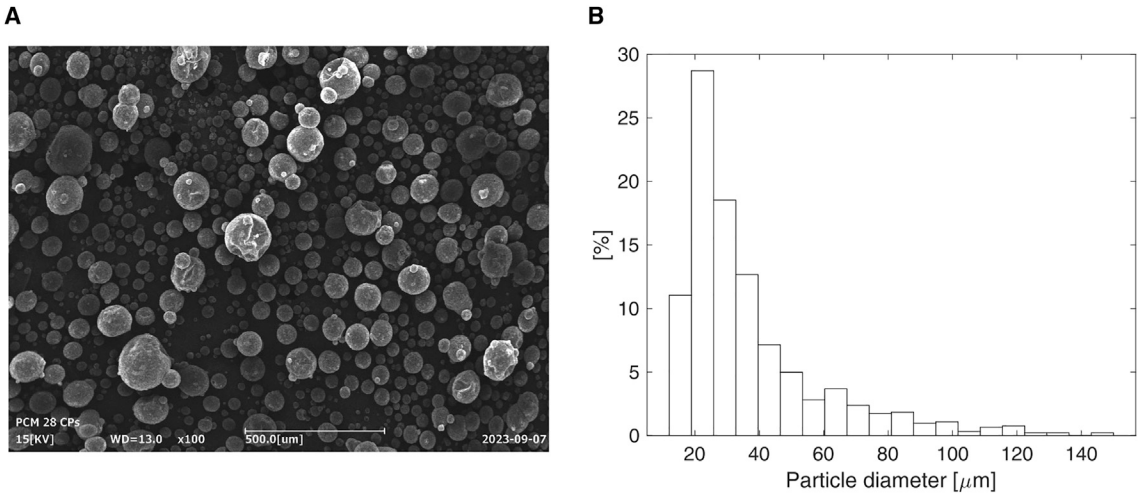

Figure 6. Example of typical micro-encapsulated paraffinic particles

(A) SEM picture of dry MPMC (PCM 28CPS by Encapsys LLC) showing their aspect. Scale bar, 500 μm, (B) Particle diameter distribution of the sample.

measure the thermo-physical and transport properties are presented and critically discussed. Moreover, some important characteristics of the slurries, such as the stability, subcooling, and hysteresis are addressed.

Thermo-physical properties

Density

In EPCM, the particle density is a combination of the densities of the core and shell materials. The core mass ratio ξ_m and volume ratio ξ_V are defined as follows:

$$\xi_m = \frac{m_c}{m_p} \quad \text{(Equation 1)}$$

$$\xi_V = \frac{V_c}{V_p} = \xi_m \frac{\rho_p}{\rho_c} \quad \text{(Equation 2)}$$

where m_c and m_p are the core and particle masses, ρ_c and ρ_p are the core and particle densities, and V_c and V_p are the core and particle volumes, respectively. The mass ratio usually depends on the production process. Konuklu et al.[45] proposed a method to evaluate the mass ratio by means of differential scanning calorimetry (DSC), comparing the latent heats of the micro-encapsulated and the bulk PCM. It is possible to define the core-to-shell ratio y as the ratio between the core mass (m_c) and the shell mass (m_s):

$$y = \frac{m_c}{m_s} = \frac{m_c}{m_p - m_c} = \frac{\xi_m}{1 - \xi_m} \quad \text{(Equation 3)}$$

According to Equation 3, the PCE is the limit case when $y = \infty$ (no shell), while for the EPCS $0 < y < \infty$. By the mass conservation, the particle density ρ_p is calculated as:

$$\rho_p = \xi_V \rho_c + (1 - \xi_V)\rho_s = \frac{(1+y)\rho_c \rho_s}{\rho_c + y\rho_s} \quad \text{(Equation 4)}$$

ρ_c being the core density and ρ_s the shell density. The mass of the particles in suspension divided by the mass of the bulk slurry (m_b) defines the particles mass ratio of the slurry φ_m:

$$\varphi_m = \frac{m_p}{m_b} \quad \text{(Equation 5)}$$

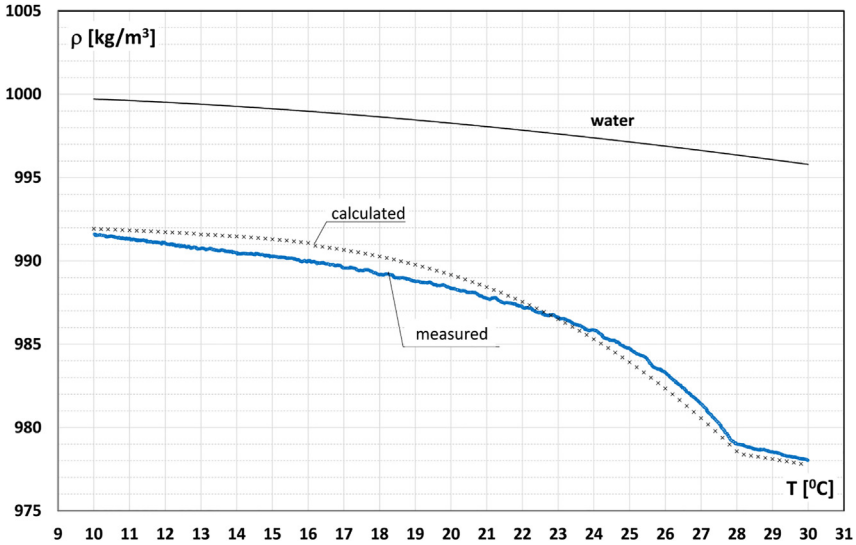

Figure 7. Water density as a function of temperature and 8.60 wt % MPCS density experimentally measured and calculated

The paraffinic core phase change (around 25°C–28°C) results in a relatively large density drop. Reproduced with permission.[47] Copyright 2020, Elsevier.

The slurry mass ratio given in Equation 5 is an important tuning parameter for the applications. The higher the φ_m, the more energy can be stored per unit mass of bulk slurry. However, this increase in slurry mass ratio also leads to higher viscosity, reducing convective heat transfer rate and increasing the required pumping power. Previous works indicate 20–30 wt % and 40–60 wt % as the maximum concentration for pumped slurry[44] and natural convection energy storage applications, respectively.[46] Once the density of the particle is known, the particle volume fraction of the slurry φ_V is defined as follows:

$$\varphi_V = \frac{V_p}{V_b} = \varphi_m \frac{\rho_b}{\rho_p} \quad \text{(Equation 6)}$$

With the same rationale as Equation 4, the density of the slurry ρ_b is obtained, with f as the subscript for the carrier fluid:

$$\rho_b = \varphi_V \rho_p + (1 - \varphi_V)\rho_f = \frac{\rho_f \rho_p}{\varphi_m \rho_f + (1 - \varphi_m)\rho_p} \quad \text{(Equation 7)}$$

With the PCS liquid at each working temperature, the slurry density can be conveniently measured by means of a hydrometer, a pycnometer, or a Coriolis mass flow meter.[47] Dutkowski et al.[47] experimentally measured the density of MPCM slurries containing water and paraffin wax particles with PMMA shells at different concentrations using a Coriolis mass flow meter around the phase change temperature. They observed a drop in density values in the phase change region, corresponding to the expansion of the melting PCM. They calculated theoretically the density trend using Equations 4 and 7 together with the thermal expansion coefficient versus temperature relationship found in the literature. Results are shown in Figure 7.

In the common cases of organic PCMs,[48] the density of the slurry is slightly lower than water. Moreover, even if the density of the PCM varies by about 15% during the phase change, the effect on the slurry density is less than 2% and can be usually neglected.[14,49] This aspect can be relevant for an energy storage application

because it reduces the amount of empty space required for the solid PCM to expand.[46]

Specific heat capacity

The specific heat capacity of the particles (c_{P_p}) and the slurry (c_{P_b}) in the absence of phase change are calculated according to the following equations based on mass-weighted averages[10]:

$$c_{P_p} = \frac{m_c c_{P_c} + m_s c_{P_s}}{m_p} = \frac{(y c_{P_c} + c_{P_s})\rho_c \rho_s}{\rho_p (y\rho_s + \rho_c)} \quad \text{(Equation 8)}$$

$$c_{P_b} = \varphi_m c_{P_p} + (1 - \varphi_m) c_{P_f} \quad \text{(Equation 9)}$$

where c_{P_c}, c_{P_s}, and c_{P_f} are the specific heat capacities of the core, shell, and carrier fluid, respectively. The specific heat of the bulk slurry can be divided into three regions,[50] defined by the finite temperature range at which the phase change process occurs. In the pre-melt and post-melt region (regions I and III, respectively) the c_{P_b} is nearly constant and equal to the mass-weighted average of the particles and carrier fluid capacities. For organic PCMs, the specific heat capacity of the slurry when the carrier fluid is water decreases with the mass concentration φ_m as the specific heats of organic PCMs are lower than that of water.[48] In the phase change region (region II), the specific heat capacity is a function of temperature, encompassing the contributions of both the phase change and the sensible heat capacities of the particles and the carrier fluid. Thus, it is referred to as apparent specific heat.

The PCMs melt in a range of temperatures defined by temperatures T_l and T_h; in general, such temperatures can differ for the melting and solidification processes due to the subcooling. The apparent specific heat capacity in the melting region is defined by the following equation[43]:

$$Q = \int_{T_l}^{T_h} c_P(T)\, dT \quad \text{(Equation 10)}$$

where Q is the latent heat related to phase change. An example of the specific heat capacity as a function of temperature is shown in Figure 8. To implement the experimental data in numerical calculations, some simplified models were proposed—i.e., left triangle, right triangle, rectangular and sine curves—as shown in Figure 9.

Alisetti and Roy[52] and Hu and Zhang[53] showed that the simplified shape assumed for the apparent specific heat capacity has little effect on the results, while the most crucial aspect is the phase change temperature range. In view of this, the rectangular shape can be adopted and the specific heat capacity in the phase change region c_{P_e} is given by[43]:

$$c_{P_e} = c_{P_b} + \frac{Q}{T_h - T_l} \quad \text{(Equation 11)}$$

where c_{P_b} is given by Equation 9. The value of the heat provided during the phase change must be measured and includes the PCM latent heat and the specific heats of the PCM, the shell, and the carrier fluid. Finally, the apparent specific heat capacity is summarized as:

$$\begin{cases} c_{P_b} & T_i < T \le T_l \\ c_{P_b} + \dfrac{Q}{T_h - T_l} & T_l < T \le T_h \\ c_{P_b} & T_h \le T \le T_f \end{cases} \quad \text{(Equation 12)}$$

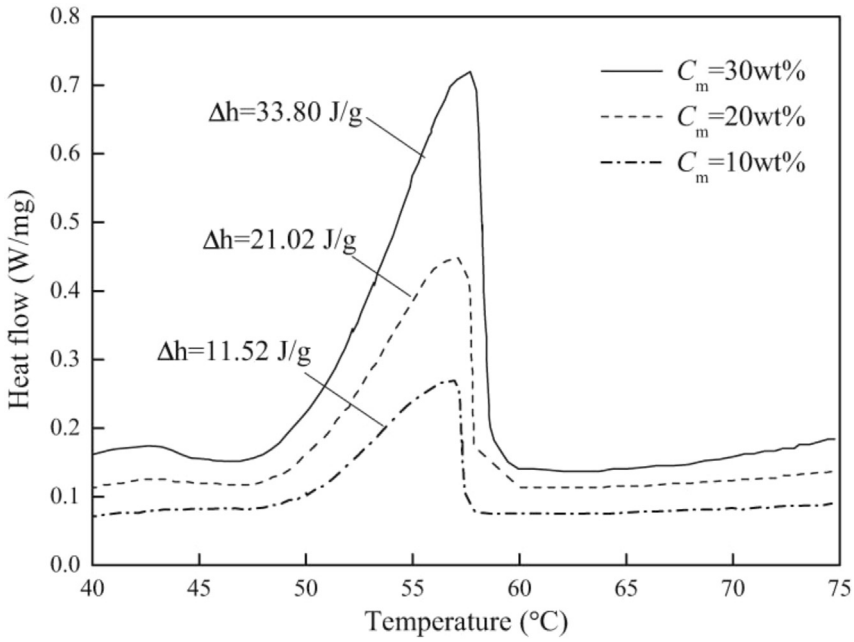

Figure 8. Output of a differential scanning calorimeter for MPCS at different concentrations
The apparent specific heat increases with concentration in the phase changing region due to the increasing latent heat (Δh). Reproduced with permission.[51] Copyright 2016, Elsevier.

Measurement of apparent specific heat capacity. Without phase change, the specific heat capacity (of the solid or liquid phase) provides the information necessary to evaluate the heat stored within the material. However, when phase change occurs, more parameters are needed to describe the phenomenon, such as phase change temperature range, phase change enthalpy, heat capacity of solid and liquid states, and subcooling degree. Pure materials have a defined phase change temperature, but PCMs are usually mixtures and thus are characterized by a melting range, as the different components melt at slightly different temperatures. The experimental thermal characterization of PCMs is performed by calorimetric measurements, which can be also applied to PCSs. Calorimetric methods applied to PCMs have been recently reviewed by Fatahi et al.[54] The most used techniques are DSC and the temperature-history (T-history) method.

DSC is widely used for PCM characterization. The most common calorimeter is the heat-flux DSC, which measures the heat adsorbed by the sample in a certain temperature range comparing the temperature variations with a reference sample placed in a symmetric position. Detailed descriptions can be found elsewhere.[7,54] Measurements can with different methods.[55]

(1) Dynamic method: the most employed, consists of heating and cooling the sample at a constant rate.
(2) Step method: heating and cooling are not continuous, but temperature is modified by small steps to allow the sample to reach thermal equilibrium.
(3) Modulated temperature method: a sinusoidal modulation is overlapped to the conventional linear ramp; this method is less common than the other two.

Despite DSC being widely used by researchers who study PCMs for heat storage, the results can be largely affected by the method used, the heating rate, and the

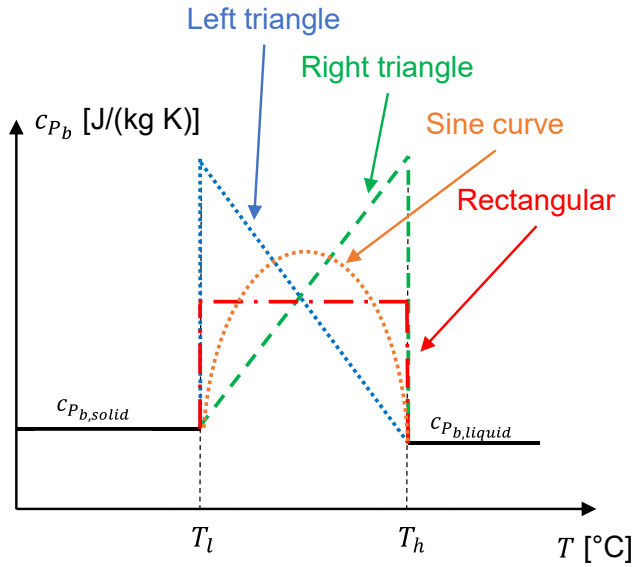

Figure 9. Simplified models of the apparent specific heat capacity as a function of temperature

sample amount. Castellón et al.[55] concluded that, with the dynamic method, there is large temperature uncertainty that can only be reduced by decreasing the heating/cooling rate, in turn affecting the enthalpy measurement uncertainty. The step method showed better accuracy and repeatability, being less sensitive to the measurement parameters. Günther et al.[56] came to the same conclusions, suggesting the step method as advisable for PCM characterization. Despite this, the dynamic method remains the most used due to its diffusion. Although, several researchers[57] concluded that thermal measurements of PCMs with the dynamic method require a heating and cooling rate of about 1 K/min. This is not consistent with the conventional standards used in DSC analysis of polymers or other substances. For example, ASTM standards recommend a heating/cooling rate of 10 K/min.[58] More details on measurement of PCMs are given in Fatahi et al.[54] Sample mass is another parameter that can influence results, as in DSC samples of 10–20 mg are used, while larger amounts can be more representative in real applications. To characterize samples up to few grams the T-history method can be suitable.

The T-history method was first developed by Zhang et al. in 1999[59] and later improved by other researchers.[60] The method is based on recording temperature versus time curves of the sample PCM and a known reference (usually water). The experimental setup consists of a tube filled with PCMs and a tube filled with the reference sample; measurements can be done with multiple PCM samples simultaneously. Samples are preheated above the melting temperature and then placed into a thermal bath at ambient temperature. The plots of temperature as a function of time of the PCM samples and the reference sample are recorded. Processing those data allows to obtain the apparent specific heat, the melting latent heat, melting temperature ranges, subcooling degree, and the effective thermal conductivity (the latter only for PCMs that show a clearly defined solid-liquid interface). Results can be represented as temperature versus time curves, but also enthalpy versus temperature[61] or effective specific heat versus temperature.[62] The main advantages of the T-history method compared with DSC are the larger samples amount (up to 15 g), the shorter measurement time, and the simple setup.[60]

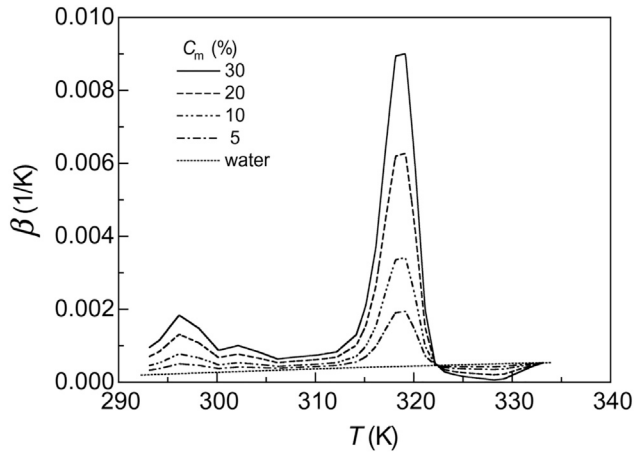

Figure 10. Volumetric expansion coefficient for MPCM slurries measured at different mass concentrations

Reproduced with permission.[64] Copyright 2003, Elsevier.

The T-history method enables measurement accuracy comparable with that of the DSC step method.[56]

Volumetric expansion coefficient

The slurry volumetric expansion coefficient β_b is defined as:

$$\beta_b = -\frac{1}{\rho_b}\left(\frac{\partial \rho_b}{\partial T}\right)_P \quad \text{(Equation 13)}$$

In thermodynamics, it represents the change in the fluid density for an increment of unit temperature at constant pressure. A method to obtain the coefficient is directly measuring it by a dilatometer. A dilatometer consists of a glass flask with a capillary of known radius at the opening as a riser tube. A millimeter scale is used to determine the liquid level in the riser tube. The glass flask is heated evenly in a water bath, and the liquid level rises as the liquid expands. Inaba et al.[63,64] measured the slurry volumetric expansion coefficient as a function of temperature for several mass concentrations (Figure 10).

The curves show maxima around the phase change range, recreating the trend of the specific heat. The expansion coefficient can be one or two orders of magnitude higher than that of water in the phase change range, increasing with mass concentration φ_m. Substituting Equation 7 in Equation 13:

$$\beta_b = -\frac{\left[\varphi_V\left(\frac{\partial \rho_p}{\partial T}\right)_P + (1-\varphi_V)\left(\frac{\partial \rho_f}{\partial T}\right)_P\right]}{\varphi_V \rho_p + (1-\varphi_V)\rho_f} \quad \text{(Equation 14)}$$

To calculate the volumetric expansion coefficient from Equation 14, the densities as a function of temperature for the carrier fluid and the MPCM particles are required. While the density function of the carrier fluid is usually known, that of the particles is more difficult to obtain. Sabbah et al.[65] proposed to interpolate the density of the particles in the melting range by using the DSC curve for scaling. The particle density is rewritten as:

$$\rho_p = \chi \rho_{p,L} + (1-\chi)\rho_{p,S} \quad \text{(Equation 15)}$$

$\rho_{p,L}$ and $\rho_{p,S}$ are the densities of the MPCM particle when the PCM is liquid and solid, respectively, and χ is the liquid fraction calculated based on the apparent specific heat capacity curve as follows:

$$\chi = \begin{cases} 0, & T < T_l \\ \dfrac{\int_{T_l}^{T} c_{p_e} dT - \int_{T_l}^{T} c_{p_b} dT}{\int_{T_l}^{T_h} c_{p_e} dT - \int_{T_l}^{T_h} c_{p_b} dT}, & T_l \le T \le T_h \\ 1, & T > T_h \end{cases} \quad \text{(Equation 16)}$$

Thus, the volumetric expansion coefficient of the MPCM particles is:

$$\beta_p = -\frac{1}{\rho_p}\left(\frac{\partial \rho_p}{\partial T}\right)_P = \frac{(\rho_{p,S} - \rho_{p,L})\left(\frac{\partial \chi}{\partial T}\right)_P}{\chi \rho_{p,L} + (1-\chi)\rho_{p,S}} \quad \text{(Equation 17)}$$

In Equation 17, the volumetric expansion coefficients of the solid and liquid phases have been neglected because they are small compared with that during the phase change. Equation 17 can be used together with Equation 14 to calculate β_b. However, the measurement of DSC is still necessary to define χ.

Transport properties

Dynamic viscosity

Viscosity is one of the critical properties of the slurry, as it influences both the pumping power when it is used as a thermal carrier and heat transfer in forced and natural convection. Higher viscosity tends to reduce the turbulence within a slurry, which, in turn, can lead to a decrease in the heat transfer coefficient. In general, the parameters that affect viscosity—besides capsule material and carrier fluid viscosity—are the particle concentration, particle size distribution, the degree of particle rupture, the melting region,[66] temperature, and shear rate.

Effect of particle concentrations and sizes. Extending the studies of Einstein's PhD thesis,[67] Vand[68] derived an expression for the dynamic viscosity of diluted aqueous suspensions of rigid spherical micro-particles homogeneously dispersed into a Newtonian fluid:

$$\frac{\mu_b}{\mu_f} = \left(1 - \varphi_V - A\varphi_V^2\right)^{-k} \quad \text{(Equation 18)}$$

where μ_b/μ_f denotes the relative dynamic viscosity of the suspension in relation to the carrier fluid and φ_V is the particle volume fraction. According to Vand, the shape factor $k = 2.5$ for rigid spherical particles while for elongated particles $k > 2.5$and remains nearly constant with the particle concentration. In the case of NPCMs/MPCMs and PCEs, particles can be approximated as spheres. In addition, in conventional NPCS/MPCS configurations, where the shells are consistently solid and directly linked to a carrier fluid, the presence of liquid cores have a negligible effect on the suspension viscosity.

The constant A considers particle-to-particle collisions, shell material properties, and particle size distributions, and therefore it must be evaluated experimentally. Vand measured $A = 1.16$ for a suspension of glass spheres of 130 μm diameter, and Charunyakorn et al.[69] used this value for their numerical calculations. However, other authors reported higher values ranging from 3.4 to 4.45 measured on MPCS, as summarized in Table 2. In general, dynamic viscosity increases with mass particle concentration and, for typical MPCSs reported in literature, it reaches about 10 times

Table 2. Constant *A* as reported in literature

Suspension	Carrier fluid	Particle size (μm)	Concentration (wt %)	*A*	Reference
Glass	water	130	0–37	1.16	Vand[68]
Paraffin core (83%) and polymer shell (17%)	water	1–30	4–32	3.4	Mulligan et al.[70]
Paraffin core and formaldehyde shell	water	2–10	0–30	3.7	Yamagishi et al.[71]
1-Bromohexadecane core and amino-plastics shell (7:1 weight)	water	10	5–28	4.45	Wang et al.[72]
Metal field's alloy nanoparticles	HFE-7100 (hydrofluoroether)	5–30 × 10^{-3}	0–30	3.5	Wu et al.[73]

Referring to Equation 28

the viscosity of water with particle concentration of 30 wt % and 100 times the viscosity of water with particle concentration of 40 wt %.

Vand's correlation stands as the only empirically validated equation employed to predict the viscosity of moderately diluted systems (see Table 2). In standard NPCS/MPCS configurations, where the shells are consistently solid and directly connected to a carrier fluid, the choice between solid and liquid cores appears to have a negligible impact on the overall viscosity. However, in practical scenarios, NPCMs/MPCMs may not exhibit perfect rigidity, sufficient dilution, or monodispersity. Furthermore, PCSs may be present in the form of liquid-liquid emulsions (PCEs), thereby lacking solid-liquid interfaces. In all these cases, the conditions for the applicability of the Vand correlation are not fulfilled. In this context, there have been substantial endeavors to encompass situations that deviate from the Einstein-Vand theory. Among the various viscosity models, the Mooney model[74] accounts for distributions of rigid spherical particle sizes up to 50 wt % concentration. On the other hand, the Krieger-Dougherty model[75] incorporates a packing factor φ_M and is more tailored for concentrated uniform rigid spherical suspensions (Equation 19). This latter has been validated across a wide range of particle suspensions and is likely one of the most employed models.

$$\frac{\mu_b}{\mu_f} = \left(1 - \frac{\varphi_V}{\varphi_M}\right)^{-\mu_b \varphi_M} \quad \text{(Equation 19)}$$

Recently, Mendoza and Santamaría-Holek[76] developed a new model that works with any arbitrary volume fraction. However, extensive testing is still required for its validation. Despite PCMs generally being perceived as rigid, certain polymeric shells may be deformable, a factor that should be considered when making viscosity predictions. Comprehensive surveys of models to calculate the viscosity of suspensions of deformable particles are given by Hsueh and Wei[77] and Faroughi and Huber,[78] where PCSs with deformable particle/fluid interfaces can be treated as oil-water emulsions.

Typically, broad size distributions are correlated to Newtonian behavior, while narrower distributions result in shear-thinning behavior.[66] The dispersion of particle sizes can be quantified by means of the span (the width of the size distribution),[79] calculated starting from the statistical distribution of the particles size according to Equation 20:

$$span = \frac{d(0.9) - d(0.1)}{d(0.5)} \quad \text{(Equation 20)}$$

where $d(0.9)$ is the size below which 90% of particles lie, $d(0.1)$ is the size below which 10% of particles lie, and $d(0.5)$ is the size below which half of the particles lie. The lower the span, the narrower is the distribution and thus a shear thinning effect is expected. Nevertheless, it has been reported that slurries with smaller particle sizes exhibit higher viscosities, as particle-particle interactions are augmented.[80] On the other side, Zhang and Zhao[81] observed, using MPCMs (10–100 μm), that for a given particle concentration and test temperature the PCS viscosity was higher for bigger particle slurries. In conclusion, there is no general model that perfectly fits all types of suspensions. Experimentation and validation are crucial to determining the most suitable model for a specific particle-liquid system and, in some cases, a combination or modification of models may be necessary for a more accurate viscosity prediction.

Effect of shear rate. Shear rate is another important variable that has a distinctive effect on the viscosity of PCSs. Previous correlations assume that particles are suspended in a Newtonian liquid phase. However, when the particle concentration reaches a certain critical value, the slurry behaves as a non-Newtonian fluid, exhibiting shear-thinning characteristics. Emulsions of water/paraffin (1–10 μm) show pseudoplastic characteristics in the concentration range of 15–75 wt %. The extent of non-Newtonian behavior becomes pronounced when the paraffin content exceeds 50 wt % and the dispersed paraffin begins solidifying.[82] Newtonian behavior was also observed for wax/acrylic and wax/PMMA MPCSs (1–100 μm) for shear rates >200 s^{-1} and mass fraction <35 wt %.[81] PCSs with 30 wt % capric acid-lauric acid and average droplet size of 1 μm present Newtonian characteristics[83] when shearing rate >50 s^{-1}. Rigid micro-capsule slurries in circular ducts tend to deviate from Newtonian behavior beyond 25 wt %.[69] Tetra-*n*-butyl ammonium bromide and clathrate hydrate slurries (5–25 wt %) present a pseudo-plastic non-Newtonian shear-thinning characteristics[84] up to 1,000 s^{-1}. Recently, McPhee et al.[66] investigated the complex rheology behavior of encapsulated phase change paraffin slurries (15–37.5 wt %) above their melting point. Their rheological response was found to be dependent on the level of shear, demonstrated by a transition from shear thickening, noticeable at relatively low shear rates (<100 s^{-1}), to shear thinning at higher shear rates. Interestingly, Cao et al.[85] and McPhee et al.[66] showed that the observed local increase in viscosity is due to particle-particle interactions at low shear stress. This increase is absent in non-encapsulated emulsions, which exhibit the typical pseudoplastic behavior.

Effect of temperature. As the temperature of liquids increases, the kinetic energy of the molecules also increases. This enhanced kinetic energy leads to more chaotic molecular motion, facilitating the flow of the liquid. As a result, viscosity tends to decrease with rising temperature in liquids. Unlike gases, liquid viscosity lacks a systematic microscopic theory. For this reason, empirical models have been developed to estimate how viscosity changes with temperature.

The Arrhenius-Andrade model is the simplest and most widely used model for temperature-dependent viscosity μ of pure liquids[86]:

$$\mu(T) = \mu_\infty e^{\left(\frac{E_a}{RT}\right)} \quad \text{(Equation 21)}$$

where E_a is the activation energy for viscous flow, R the universal gas constant, T is the absolute temperature, and μ_∞ the viscosity at $T = \infty$. Other commonly employed models for polymer-like liquid melts are the Vogel-Tammann-Fulcher[87] and Williams et al.[88] models.

Further the rheological characteristics of PCSs are more complex than those of pure liquids, they are still significantly influenced by operating temperature, often resulting in a decrease in viscosity as temperature rises. In addition, the nano/microstructure of slurry particles might break down at elevated temperatures, potentially causing a gradual viscosity reduction during both slurry operations and storage.[83] Zhang and Zhao[81] conducted rheological investigations on slurry composed of an MPCM with a paraffin core and a shell comprising crosslinked acrylic polymer. Their research revealed that, with a consistent mass fraction of 35 wt % in a water-based fluid, viscosity decreased with temperature. More recently, Dutkowski and Fiuk[89] performed a study on the viscosity of commercially purified paraffins enclosed in polymethylmethacrylate shells in water using different heating rates (ranging from 0.1°C/min to 1.2°C/min). The authors observed that the phase transformation of the core material significantly impacts the measured viscosity values, causing an increase in the viscosity in the phase change region.

Measurement of dynamic viscosity. The PCS viscosity is typically referred to as dynamic viscosity (μ), a measure of a fluid resistance to flow in the time domain, defined by the ratio of shear stress (τ) to shear rate ($\dot{\gamma}$). This rheological property is measured using a rotational rheometer or "viscometer," which precisely controls a spindle or bob immersed within the PCS sample. The rheometer induces rotational motion, applying shear stress to the material. As the spindle rotates at various shear rates, the rheometer measures the resulting torque and angular displacement, providing detailed information on the material viscosity as a function of shear. Some rheometers include temperature control features, offering insights into the material response across a range of temperatures.

Complex viscosity (μ^*) is another type of viscosity used for more advanced rheological analysis performed in the frequency domain using plate-plate oscillatory rheometers. This physical property accounts for both the elastic and viscous responses of viscoelastic materials like polymer melts. Note, while dynamic viscosity and complex viscosity are essentially the same for Newtonian fluids, they can differ for more complex materials such as PCS, particularly at high particles content. This difference is crucial to consider, as energy and mass transport models are generally expressed in terms of dynamic viscosity rather than complex viscosity.

Thermal conductivity

The thermal conductivity of the particle can be evaluated by means of the composite sphere method[90] to consider the contribution of the shell:

$$k_p = \frac{k_s k_c \sqrt[3]{\frac{y\rho_s}{y\rho_s+\rho_c}}}{k_s+\left(1-\sqrt[3]{\frac{y\rho_s}{y\rho_s+\rho_c}}\right)k_c} \quad \text{(Equation 22)}$$

where k_c is the core conductivity, k_s the shell conductivity, and k_p the particle conductivity. Several models have been proposed to calculate the thermal conductivity of the bulk slurry k_b, which can be evaluated using the Maxwell's formula[91] for suspended spherical particles (k_f is the carrier fluid conductivity):

$$k_b = \frac{2k_f+k_p+2\varphi_V(k_p-k_f)}{2k_f+k_p-\varphi_V(k_p-k_f)}k_f \quad \text{(Equation 23)}$$

Maxwell's model is the simplest one, assuming spherical particles and depending only on thermal conductivities of the fluid and particles and their volume fraction. The thermal conductivity of a PCS containing paraffin-based MPCM with PMMA shell

in a water-glycol solution was measured by Dutkowski and Kruzel.[92] Measurements were carried out in the 10°C–40°C range with mass fraction up to 43 wt %. They showed that Maxwell's equation predicted the thermal conductivity within 20% accuracy. In the phase change region, they measured a peak of thermal conductivity, which is not the true value due to the imperfection of the measurement method. Successive models take in account also the particle shape,[93] particles interactions,[94] contact resistance,[95] particles size and interfacial properties.[96] Comprehensive surveys of the developed models to calculate the conductivity of fluids with suspended particles are given by Proghelof et al.[97] and Vatani et al.[98]

Equation 23 and the more complex models mentioned above are valid in static conditions. The effective thermal conductivity of the slurry (k_e) is higher due to the interactions between the particles and the carrier fluid, namely, micro-convection. According to Sohn and Chen,[99] solid particles within a shear flow rotate with a rate proportional to the shear rate $\dot{\gamma}$. The particles drag the surrounding fluid producing eddies of the same order of particle diameter magnitude. Such eddies induce micro-convective effects that are proportional to the surface velocity $\dot{\gamma} d_p$ and the eddies length scale d_p – being d_p the size of the solid particles. The particle Peclet number Pe_p is a measure of the convection at eddies scale compared with conduction:

$$Pe_p = \frac{\dot{\gamma} {d_p}^2}{a_f} \quad \text{(Equation 24)}$$

where a_f is the thermal diffusivity of the surrounding fluid. With Pe_p sufficiently high, micro-convection becomes an additional transport mechanism with respect to molecular conduction. Charunyakorn et al.[69] proposed the following expression for the effective thermal conductivity:

$$\frac{k_e}{k_b} = 1 + B\varphi_V {Pe_p}^m \quad \text{(Equation 25)}$$

The values of B and m depend on the particle Peclet number:

$$\begin{cases} B = 3.0 \;\; m = 1.5, & Pe_p < 0.67 \\ B = 1.8 \;\; m = 0.18, & 0.67 \leq Pe_p \leq 250 \\ B = 3.0 \;\; m = 1/11, & Pe_p > 250 \end{cases} \quad \text{(Equation 26)}$$

Micro-convection may be significant in forced convection, as the shear rate is higher, while can be negligible for small shear rates, such as in natural convection.[65] Moreover, Yamagishi et al.[71] showed that for particles less than 100 μm the micro-convective effect can be negligible.

Additives such as graphene and carbon nanotubes can be also added to increase the thermal conductivity of particles while preserving energy storage capability.[100]

Hysteresis and subcooling

PCSs properties can exhibit different behaviors of the material under heating or cooling, and this is especially visible in the enthalpy-temperature curves, namely hysteresis. It is generally more pronounced in inorganic PCM than organic ones. Hysteresis originates from multiple sources, but the most common in PCMs is the subcooling (also named supercooling or undercooling). Subcooling occurs when the PCM is cooled to a temperature below the melting point before it starts to crystallize. Subcooling is a property of the material but also strongly related to the scale, as it can be negligible in macroscopic geometries while arising in microscopic geometries.

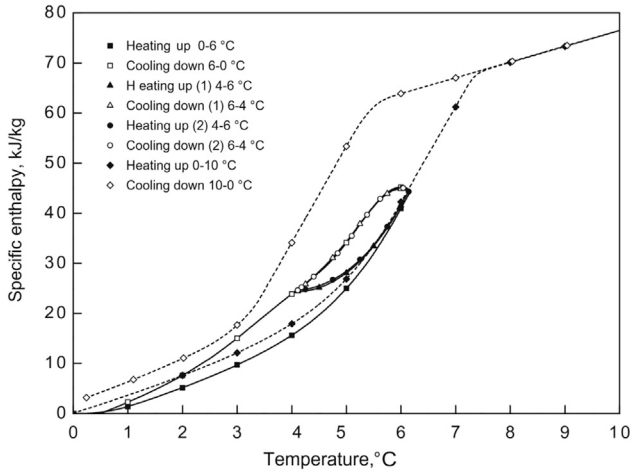

Figure 11. Specific enthalpy measured during several heating and cooling cycles in the phase change temperature range

Hysteresis patterns are recognizable since the curves are dependent on the previous heating/cooling cycles. Reproduced with permission.[102] Copyright 2010, Elsevier.

The origin of the subcooling can be explained with the classical nucleation theory. The solidification process consists of a nucleation process and a later growth of the stable nucleus. Nucleation can be homogeneous, when initiated from the bulk phase, and heterogeneous, when initiated from some defects or inclusions that make the properties locally non-homogeneous. The latter is the main nucleation process occurring in practice, as requires less energy to evolve. Heterogeneous nucleation develops from walls or defects of the material. In the case PCM particles, the smaller the particle, the fewer nucleation sites are present in the material, leading to a general increase in required subcooling to activate nucleation. Thus, reducing the particle size will increase the subcooling level.[9]

Many authors have studied the subcooling problem and proposed techniques to mitigate this issue. One of the most commonly used methods in emulsions and micro-capsules is the addition of nucleators,[20] which can have similar or different chemical composition than the PCM. In emulsions, surfactants can also act as nucleators at the droplet interface, especially for larger ones.[101]

Hysteresis can be an issue in PCS. Diaconu et al.[102] measured the hysteresis caused by the subcooling in an MPCS at 45 wt % within the phase change region (4°C–7°C) under several heating and cooling cycles. As shown in Figure 11, the subcooling degree and the enthalpy-temperature dependence vary with the temperature history, making the mathematical description of the slurry more complicated.

Stability

PCS must maintain their properties over thousands of charge/discharge cycles in applications. This means that the fluid must remain homogeneous, and particles must retain their shape. The following instabilities can occur[14,44].

(1) Creaming or sedimentation: the different densities between the particles and carrier liquid, and the action of gravity, can lead to precipitation of particles when their density is higher than that of the liquid or floating when particles are less dense than the liquid. Smaller particles are less affected by gravity, as Brownian motions can partially compensate for them.

(2) Flocculation: in emulsions, particles adhere to form larger clusters.
(3) Coalescence: in emulsions, it is the fusion of liquid drops resulting in larger ones.
(4) Ostwald ripening: in emulsions, smaller droplets tend to solubilize in the carrier liquid and then deposit on the interface of the bigger droplets. Ultimately, the effect is that smaller droplets disappear, and bigger droplets increase the size.
(5) Phase inversion: in emulsions, the carrier and suspended liquid phases can invert.

The above instability mechanisms can all occur in emulsions, while the protective shell of micro-capsules prevents most of them. The use of surfactants is necessary in emulsions and their stability in the long term must be guaranteed. Microencapsulated can show creaming/sedimentation due the particles size and the ratio between buoyancy and Brownian forces and agglomeration.[9] Density separation depends on buoyancy prevailing over Brownian motion, and its evaluation involves assessing the Peclet parameter *Pe*[103]:

$$Pe = \frac{\pi \Delta \rho g d_p^4}{24 k_B T} \quad \text{(Equation 27)}$$

where $\Delta\rho = \rho_f - \rho_p$ represents the difference in density between the aqueous medium and the particle, g is the gravitational constant, d_p the capsule diameter, k_B the Boltzmann's constant, and T the absolute temperature of the PCS. A $Pe > 1$ indicates the dominance of gravitational forces over Brownian motion, whereas a $0 < Pe < 1$ indicates that Brownian motion prevails over gravitation. Consequently, the latter condition must be avoided to reduce creaming and agglomeration phenomena.

The major risk for the long term stability of EPCM consist of the shell rupture. Yamagishi et al.[104] reported that simple agitation of the micro-capsules does not produce shell rupture. Furthermore, to avoid the shell rupture and enable the slurry to operate over thousands of cycles, it is important to prevent abrupt pressure changes. In general, larger particles are more susceptible to rupture, while, as discussed above, smaller particles require higher subcooling to initiate the solidification. Gschwander et al.[105] found that centrifugal pumps inflict the least damage to the capsules; Kong et al.[106] used a progressing cavity pump and found that particles showed no significant damage after more than 120,000 cycles.

In conclusion, creaming/sedimentation and shell rupture are the most common issues of micro/nano-encapsulated slurries. Reducing the size of particles can solve the problem of creaming/sedimentation and increase the shell resistance under stressing conditions (e.g., pumps), but it will increase the subcooling degree of the PCM. Emulsions could be affected also by coalescence, flocculation, Ostwald ripening, and phase inversion, that make them potentially unstable with time.

NATURAL CONVECTION HEAT TRANSFER

Thermal storage involves the process of charging and discharging energy. The heat is transferred from the bulk to the secondary heat transfer fluid and vice versa due to heat exchangers, that usually consist of tubes in different configurations. In the absence of bulk fluid agitation, the limiting factor to the energy transfer is represented by natural convection on the external walls of the tubes. Moreover, convective motion of bulk fluid causes recirculation and mixing of the fluid, influencing the stratification and the performances of the storage.

In thermofluid dynamics, Rayleigh number *Ra* is a dimensionless number associated with buoyancy-driven flow. It is defined as the ratio of the timescale for thermal transport via diffusion to the timescale for convective thermal transport. It includes the temperature difference between the wall and the bulk fluid, $(T_w - T_b)$, the gravity acceleration (g), a characteristic length that depends on geometrical configuration (L), and the thermo-physical and rheological properties of the fluid. *Ra* number determines whether buoyancy-driven natural convection plays an important role in heat transfer.[107]

$$Ra = \frac{\rho_b{}^2 c_{P_b} |\beta_b (T_w - T_b)| L^3 g}{\mu_b k_b} \quad \text{(Equation 28)}$$

The Nusselt number *Nu* is calculated as a function of *Ra*, according to traditional dimensional analysis and correlations. The heat transfer coefficient h_c is then determined as:

$$Nu = \frac{h_c L}{k_b} = f(Ra) \quad \text{(Equation 29)}$$

Considering as reference the case of organic MPCM suspended in water, the thermal conductivity of the slurry is generally reduced with respect to pure water, while dynamic viscosity is increased. On the other hand, the apparent specific heat and the volumetric expansion coefficient are higher than pure water in the phase change region. Consequently, a certain reduction of heat transfer is expected compared with pure water, with the possibility of improved performance around the phase change region. In any case, the potential heat transfer reduction can be acceptable, as there is a beneficial increase in the heat stored due to the phase change.

To assess performances of and correctly model the storage with PCS, it is crucial to have a good understanding of the heat transfer with natural convection. Despite the importance of this aspect, in literature the number of studies is still limited and condensed in the past two decades. In the following section, the scientific works dealing with natural convection of PCS are reviewed. These are divided according to the geometrical configuration investigated and listed in Table 3. In particular, the rectangular cavity is a fundamental geometric shape that comprises of two adiabatic walls, and two walls at different fixed temperatures. This geometry can be simplified into a two-dimensional model for numerical investigations. Despite its simplicity, it is often adopted to characterize and model the natural convection heat transfer. Helically coiled and horizontal tubes heat exchangers are widely used in TES applications due to their compactness, efficiency, and practicality.[108] For these reasons, many of the reviewed articles focus on these configurations.

As regards forced convection, details on this heat transfer regime with PCS can be found in other specific reviews.[9,10,42–44]

Rectangular cavity

One of the simplest geometries to study natural convection consist of two plates, one of which heated and the other cooled. The first studies on natural convection with PCS focused on this geometry.

Inaba et al.[64] experimentally studied the natural convection in a rectangular cavity that was heated from below and cooled from above. The cavity length was 120 mm, and the height was adjusted to vary the aspect ratio (*AR*). The slurry was

Table 3. Studies on natural convection in PCS

	Type of study	Geometry	Carrier fluid	Particle size (μm)	Phase change region (°C)	Concentration (wt %)	Reference
PCM emulsion	experimental	rectangular cavity	water/surfactants 5%	<1	40–50	0–30	Inaba et al.[64]
	numerical	rectangular cavity	water/surfactants 5%	not provided (n.p.)	40–50	30	Inaba et al.[109]
	experimental	vertical coil	water/surfactants	1 (avg.)	30–50	60	Delgado et al.[110]
	experimental	rectangular cavity	water/alcohol/ surfactants	2.7–3.48 (avg.)	28.2	10–20	Morimoto and Kumano[111]
MPCM	experimental	vertical coil	water	5–10	60	0–50	Heinz and Streicher[46]
	numerical	rectangular cavity	water	n.p.	25–35	0–40	Inaba et al.[63]
	experimental	vertical coil	water	2.24 (avg.)	2–7	45	Diaconu and co-workers[102,112]
	experimental	vertical coil	water	2–8	65	25–50	Huang et al.[113]
	experimental	rectangular cavity	water	0–4.5	25–38	10–40	Zhang et al.[114]
	numerical	rectangular cavity	water	n.p.	21–30	0–25	Sabbah et al.[65]
	experimental	rectangular tank	water	n.p.	25–38	10–40	Zhang et al.[115]
	experimental	horizontal tube	water/propanol/ alginate	10–40	50.85–58.11	0–30	Wang et al.[51]
	experimental	rectangular cavity	n.p.	n.p.	n.p.	40	Li et al.[116]
	experimental	horizontal bundle	water	1.85 (avg.)	11.9–16	45	Allouche et al.[117]
	numerical	horizontal bundle	water	1.85 (avg.)	11.9–16	45	Allouche et al.[118]
NPCM	numerical	square cavity	n.p.	<1	n.p.	<5	Ghalambaz et al.[119]
	numerical	square cavity	water	<1	32	<5	Hajjar et al.[120]
	numerical	vertical surface	water	<1	n.p.	<5	Ghalambaz et al.[121]

an emulsion made of water, surfactants, and paraffin wax particles with size less than 1 μm and concentration up to 30 wt %. The phase change region was measured and ranged from 40°C to 50°C. Being an emulsion, the slurry showed shear-thinning behavior, thus the Rayleigh number for a non-Newtonian fluid was used to generalize the experimental results:

$$Ra_H = \frac{\rho_{b,0}\overline{\beta_b}(T_H - T_C)H^{2n+1}g}{Ka_{b,0}{}^n} \quad \text{(Equation 30)}$$

where K is the consistency index and n is the pseudoplastic index of the power law model of the fluid.[122] H is used as a characteristic length according to Ozoe and Churchill.[123] The subscript 0 for the density and thermal diffusivity indicates that these are calculated at the reference state (the temperature just before PCM melting begins). The temperature difference between the top cooling plate (T_C) and the temperature of the bottom plate (T_H) was used. The value of the volumetric expansion coefficient $\overline{\beta}$ was determined as the integral averaged value from the temperature of the top plate to the temperature of the bottom plate:

$$\overline{\beta_b} = \frac{\int_{T_C}^{T_H}\beta_b(T)dT}{T_H - T_C} \quad \text{(Equation 31)}$$

The top and bottom horizontal plates were kept at constant temperature by means of a heater and a cold plate. The authors measured the heat transfer coefficients and Nusselt number separating the process into the three stages: PCM in solid phase, in phase changing, and in liquid phase.

Some of the heat transfer coefficients for the PCM in solid phase and phase changing phase are shown in Figure 12. In all cases, the heat transfer coefficients are reduced with increasing mass concentration. The heat transfer coefficient for 30 wt % concentration remains the same for increasing plates temperature difference, meaning that the natural convection is completely suppressed due to high viscosity. However, in

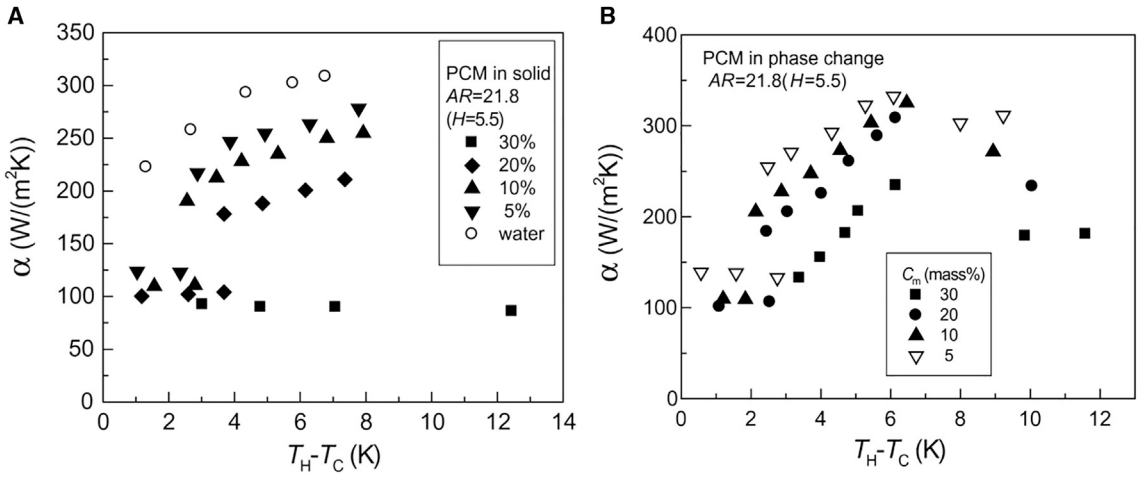

Figure 12. Heat transfer coefficients of water and slurries at different concentrations

(A) The PCM core is in solid phase, (B) the PCM core is in phase changing. Reproduced with permission.[64] Copyright 2003, Elsevier.

the phase changing region there is a maximum even for the highest mass concentration, because of the phase change contribution on the heat transfer process.

The experimental results in the solid and liquid phases were correlated according to the equation $Nu = C \cdot Ra_H^{1/(3n+1)}$. In the phase changing region, the only dependence of Rayleigh cannot reflect the intensity of natural convection for PCS. The phase change process must be considered. The following modified Stefan number *Ste* was proposed and included into the correlation:

$$Ste = \frac{c_{P_{b,0}}(T_h - T_l)}{\int_{T_l}^{T_h} c_{P_b} dT} \quad \text{(Equation 32)}$$

where $c_{P_{b,0}}$ is a reference apparent specific heat at 40°C (at the boundary of the phase change region). The Stefan number is the ratio of the sensible heat to the latent heat involved in the heat transfer process, and it is usually used in two-phase heat transfer phenomena. To the authors knowledge, this is the only attempt to correlate Nusselt number for MPCS natural convection including Stefan number. The correlation derived in the paper are reported in Table 4.

The typical empirical correlation for an enclosure filled with Newtonian fluid, in laminar flow, and neglecting the effects of the side walls is given by Globe and Dropkin[107,124] in the form: $Nu = 0.069 \cdot Ra_H^{1/3} Pr^{0.074}$. The expressions in Table 2 also include the effect of fluid rheology, particles concentration, side walls, and phase change. Nusselt number increased in the phase change region and with mass concentration; however, being the thermal conductivity smaller than that of pure water, the overall heat transfer coefficients decreased with increasing PCM concentration. When *Ste* = 1 the contribution of the phase change in the heat transfer process is negligible.

Numerical studies were also conducted by Inaba et al.[63,109] for a similar slurry, geometry, and conditions of the previous work. Emulsion and MPCM were used in the two studies, but the discussion was similar. It has been shown that the phase change process contributes to increase the heat transfer coefficients. Nevertheless, heat transfer coefficients decreased with increasing mass concentration, as suppression of natural convection due to viscosity exceeds the enhancement

Table 4. *Nu* correlation for a rectangular cavity

PCM state	Nusselt number	Conditions for validity
PCM in solid phase	$Nu = 0.22(1 - 2.7\varphi_m e^{-0.063AR}) Ra_H^{1/(3n+1)}$	$1\times10^3 < Ra_H < 6\times10^6$ $0 < \varphi_m < 30$ wt % $5.0 < AR < 22.0$
PCM in phase changing	$Nu = 0.22(1 - 2.7\varphi_m e^{-0.025AR}) Ra_H^{1/(3n+1)} Ste^{-1/4}$	$5\times10^2 < Ra_H < 2\times10^7$ $0 < \varphi_m < 30$ wt % $5.0 < AR < 22.0$
PCM in liquid phase	$Nu = 0.22(1 - 2.0\varphi_m e^{-0.02AR}) Ra_H^{1/(3n+1)}$	Ra_H validity range not provided $0 < \varphi_m < 30$ wt % $5.0 < AR < 22.0$

According to Inaba et al.[64]

of the phase change process. In the paper, a correlation obtained from the numerical results was proposed in the PCM phase changing region (in the range $10^3 < Ra < 6 \cdot 10^6$):

$$Nu = (1.1 - 0.78n) Ra_H^{1/(3.5n+1)} Ste^{-(1.9-1.65n)} \quad \text{(Equation 33)}$$

Morimoto et al.[111] experimentally investigated the natural convection of an n-octadecane emulsion with 10 and 20 wt % in a rectangular cavity with an aspect ratio ranging from 2 to 4. Temperatures were measured by 30 thermocouples. They observed an increase in the Nusselt number in the phase-changing region, which was more pronounced for the 20 wt % concentration. Moreover, they found a dependency also on the cavity aspect ratio, with the best performance observed for an aspect ratio of 3.

Zhang et al.[114] performed some experiments on a rectangular enclosure heated from below as.[64] The slurry used was obtained by mixing water and MPCM in concentrations ranging from 10 to 40 wt %. The diameter of the particles was distributed between 0 and 4.5 μm with average diameter of 0.78 μm, with phase change region within the range 25°C–38°C. The experimental conditions were like those reported in Inaba et al.[64] Temperature distributions and *Nu*-*Ra* plots were used to evaluate the heat transfer performances. Only the phase change region was investigated. Results were comparable with those of Inaba et al.[64]

Zhang et al.[115] also evaluated the heat storage capacity of the enclosure for different mass PCM concentrations: the heat storage capacity increased with mass concentration, and the storage completion time increased with mass concentration and height. Due to the limited experimental data, no generalization on the natural convection mechanism has been carried out; however, a maximum of the heat transfer coefficient was measured in the phase change region, and a reduction of the heat transfer coefficient occurred with increasing mass concentration.

Sabbah et al.[65] numerically investigated the natural convection of MPCM in a rectangular cavity with vertical hot and cold plates. In this configuration, natural convection occurrence is favored. Properties of the MPCM slurries were measured (specific heat and volumetric expansion coefficient) and calculated (thermal conductivity, density, and viscosity). Subcooling effect was neglected. Differently from the cases of rectangular enclosure heated and cooled from the horizontal plates, in the case of the vertical heated wall the heat transfer coefficients and the Rayleigh number increased with mass concentration until reaching a plateau, as illustrated in Figure 13.

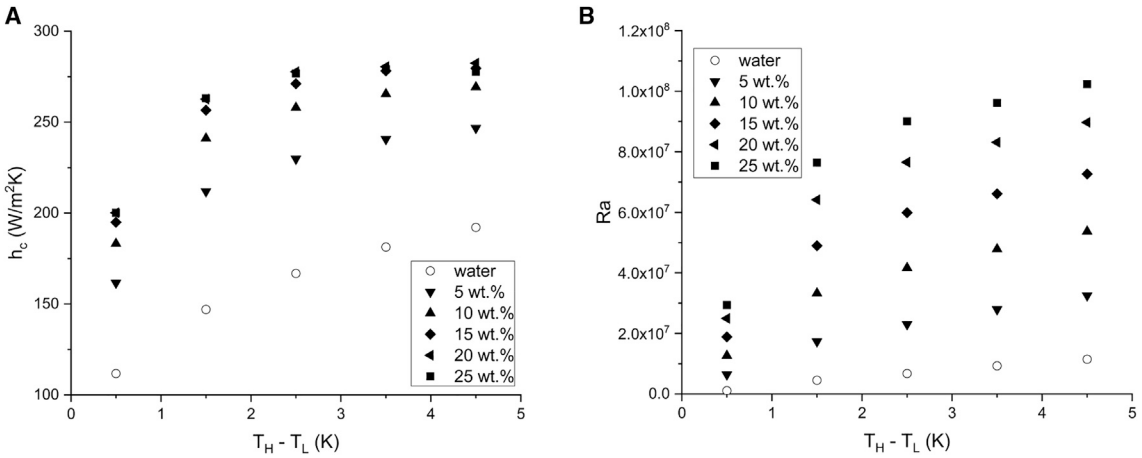

Figure 13. Natural convection in a rectangular cavity with vertical walls

Heat transfer coefficient (A) and Rayleigh number (B) as a function of temperature difference for slurries at different mass fractions. Plots are developed from collected data.[65]

According to these studies, heat transfer coefficient is influenced by the following factors.

(1) Apparent specific heat capacity: heat capacity increases with mass concentration and enhance the heat flux between the walls, due to latent heat. The effect is limited to the phase change region.
(2) Volumetric expansion coefficient: the buoyancy effect is increased due to the expansion coefficient, which is higher for higher mass concentrations. This effect appears in the phase change region as well.
(3) Viscosity: the increased viscosity of the slurry reduced circulation suppressing natural convection and decreasing the heat transfer. Viscosity increases with mass concentration and keep its value within the PCM solid, phase changing and liquid regions.
(4) Thermal conductivity: the reduction of thermal conductivity decreases the heat flux between the walls. For low shear-rate flows and small particles, the effective thermal conductivity is basically the bulk one.

Thus, the competing effects of the above factors determine the effective enhancement or reduction of the heat transfer. A key parameter is the mass concentration: according to Sabbah et al.,[65] increasing the mass concentration above 20 wt % could result in reduced heat transfer in the considered configuration.

Note that no experimental data were used to validate the numerical results, as there were no published experimental data or correlations available. To the authors' knowledge, this gap still exists in literature.

Li et al.[116] studied the natural convection in a rectangular cavity with a heated wall varying its inclination (vertical, 90° and 180°) and filling with bulk PCM, dry MPCM particles and slurry up to 40 wt % concentration. The slurry showed advantages in terms of heat transfer compared with the other systems.

Vertical helical coil

One of the most common heat exchangers in conventional storage tanks is the helical coil tube. Thus, a part of the studies focused on this geometry. Usually, the

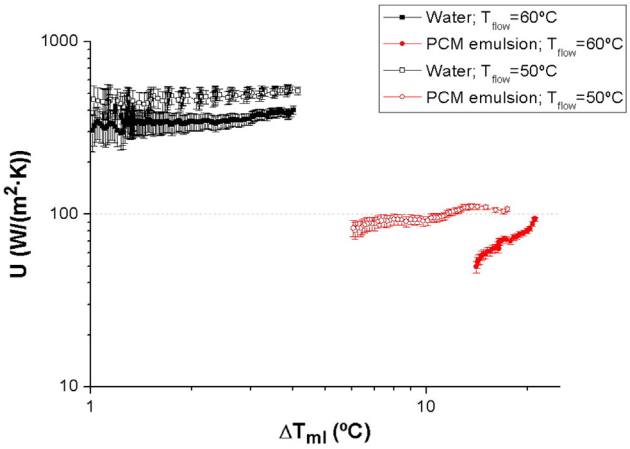

Figure 14. Heat transfer coefficients of water and 60 wt % emulsion
Error bars represent measurement uncertainty. Reproduced with permission.[110] Copyright 2015, Elsevier.

secondary fluid that flows inside the tube is water; being forced convection, the heat transfer coefficient of the internal side of the tube is much higher than the external one and the conductive thermal resistance of the metal tube wall is negligible due to its small thickness and high thermal conductivity.

Delgado et al.[110] tested a 60 wt % emulsion in a 46 L commercial tank used as TES, comparing its heat transfer and storage performance with respect to water. The mean diameter of the particles was 1 μm and the phase change region between 30°C and 50°C They found that the heat transfer rates were three to five times smaller compared with water due to the high viscosity of the slurry (see Figure 14). However, the energy storage density was 34% higher than that of water, indicating that the PCS can be a promising solution for future energy storages.

Heinz and Streicher[46] compared different modes to integrate the PCM into storage tank. A cylindrical storage with a volume of 200 L was built and filled with PCS by BASF with melting point around 60°C with mass concentrations ranging from 20 to 50 wt %. A vertical helical coil tube was used to charge and discharge the storage tank. Natural convection heat transfer coefficients of the coil were measured as a function of charging/discharging time. It was reported that all the slurries showed a decreased heat transfer with respect to pure water.

Diaconu et al.[102,112] performed an experimental investigation of the natural convection of a helical coil heat exchanger immersed within a 45 wt % slurry. The MPCS is composed of water and micro-capsules of Rubitherm RT6, with mean diameter of 2.24 μm and phase change region ranging from 2°C to 7°C. The heat exchanger was made of a 16 mm external diameter copper tube, with a helix diameter of 140 mm and a pitch of 37 mm. The helical tube was inserted in a tank of 550 mm height and 240 mm diameter (aspect ratio 2.3). Thermo-physical properties of the slurry were measured. A certain degree of subcooling was observed in the DSC curves, resulting in a hysteresis-like behavior that complicates the development of correlations, as the dependence of properties on temperature is not unique.

The Nusselt number with the tank filled with pure water was correlated to the Rayleigh number (Ra_L) calculated considering the length of the tube (L):

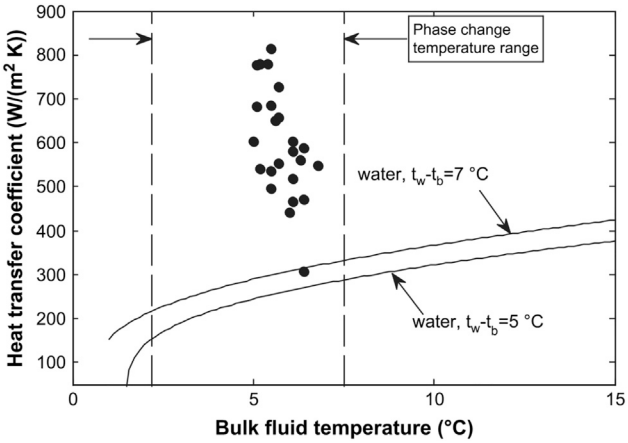

Figure 15. Comparison of heat transfer coefficients for water and slurry in the phase change temperature range

Reproduced with permission.[112] Copyright 2010, Elsevier.

$$Nu_{L,water} = 0.802 Ra_L^{0.278}, 10^{11} < Ra_L < 10^{13} \quad \text{(Equation 34)}$$

Then, the heat transfer coefficients of the slurry ($h_{c,slurry}$) were compared with the ones of water under the same conditions (wall and bulk temperatures), obtaining the following relation - heat transfer coefficients are expressed in W/(m^{2}K):

$$h_{c,slurry} = -1.797 h_{c,water} + 1180 \quad \text{(Equation 35)}$$

The above relation is valid for water heat transfer coefficients in the range 150–550 W/(m^{2}K). Heat transfer coefficients of water drops in the vicinity of 4°C, because of the maximum of density for that specific temperature. Thus, the slurry shows heat transfer coefficients up to five times higher in the temperature range between 4°C and 8°C, as shown in Figure 15. MPCS shows great potentiality in cooling applications (around 4°C).

Huang et al.[113] realized an experimental apparatus configured as a conventional water storage cylinder and performed some experimental tests with water and micro-encapsulated slurry at different volume concentrations. The micro-capsules showed phase change temperature around 65°C and their size ranged from 2 to 8 μm. MPCM was mixed with water in volume concentration of 25%, 35%, and 50%. The heat exchanger was made of a 22 mm external diameter copper tube, with a helix diameter of 198 and 400 mm height. The helical tube was inserted in a tank of 270 mm diameter and 1,000 mm height (aspect ratio 3.7). To simulate a solar collector, water at 70°C was circulated into the serpentine charging the storage tank; temperatures in various locations were collected by means of thermocouples. Temperatures evolution and energy stored as a function of time were evaluated, while less attention has been paid to the heat transfer process. Anyway, results showed that slurries with 50 vol % concentration result in a large suppression of natural convection, leading to low heat transfer rates and fluid mixing. Thus, they were unadvised as heat storage in the studied configuration, while different solutions (fins, different heat exchangers) are suggested for further studies.

Bai et al.[125] studied a cylindrical tank filled with 25 wt % mass concentration slurry made of water and micro-capsules with phase change temperature around 18°C and average diameter of 12.5 μm. The tank was 500 mm height and 300 mm

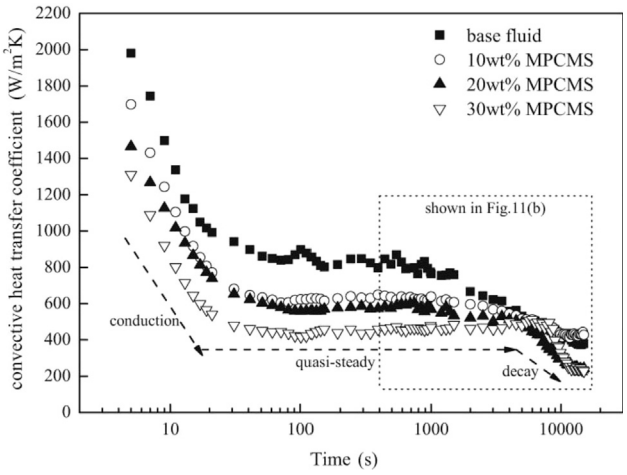

Figure 16. Heat transfer coefficients for the base fluid and MPCM slurries at different concentrations

Reproduced with permission.[51] Copyright 2016, Elsevier.

diameter t (aspect ratio 1.67) and two helical coil heat exchangers of 15 mm external diameter and 11 m length served to charge and discharge the tank. Moreover, a stirrer was also used to add some forced convection and improve the heat transfer.

External horizontal tube

Wang et al.[51] constructed an experimental rig to investigate the heat transfer characteristic of a horizontal tube immersed within an MPCS with mass concentration ranging from 10 to 30 wt %. Capsules were made of N-hexadecane (phase change range from 50.85°C to 58.11°C) with diameter ranging from 10 to 40 μm. The carrier fluid consisted of a solution of water-propanol with alginate additives, to match the density of particles and allow the suspension stability for more than 7 days. The slurries behaved as Newtonian fluid, with the viscosity increasing with mass concentration. The effects of mass fraction, inlet temperature, and mass flow of the heat source were studied. Results showed that the convective heat transfer decreased with concentration due to the increase of viscosity (see Figure 16), and that the increase of inlet temperature and mass flow rate of the heat source were beneficial for the heat transfer process.

Bundle of horizontal tubes

Allouche et al.[117] evaluated the heat transfer and cold storage characteristics of a horizontal tank with two heat exchangers realized with a bundle of horizontal tubes. The bundles consisted of a central tube with six surrounding at 22 mm pitch, external diameter of the tubes was 16 mm and their length 400 mm. The heat transfer coefficient and the relation between *Nu* and *Ra* was evaluated for the slurry and compared with pure water. The results were in accordance with the findings of Inaba et al.[64]: outside the phase change region, the Nusselt number is independent on Rayleigh, meaning that natural convection is suppressed. However, in the phase change region, *Nu* number showed an increase due to the convective motions (Figure 17). Despite higher *Nu* numbers, the heat transfer coefficient is lower than that of water as the thermal conductivity is reduced.

Closing remarks on natural convection

The literature review highlights important aspects of the different configurations studied. In the following, a comparison between water and aqueous PCS in terms of natural convection heat transfer is discussed.

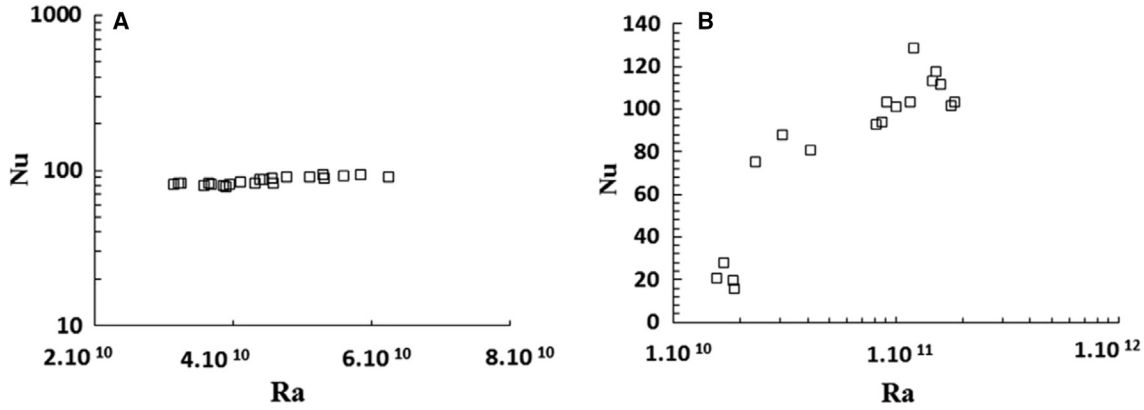

Figure 17. Nusselt versus Rayleigh plots of a slurry

(A) The PCM is in liquid state. (B) The PCM is in the phase change region. Reproduced with permission.[117] Copyright 2015, Elsevier.

Suspending particles in a carrier liquid produces a certain increase in viscosity, which can result in non-Newtonian behavior. The viscosity increases non-linearly with particle concentration. This effect appears to be dependent solely on the presence of particles and is therefore universal across all materials. An increase in viscosity leads to a suppression of buoyancy-induced motion, which in turn deteriorates convective heat transfer.

The introduction of particles into the carrier liquid affects thermal conductivity, resulting in a sort of averaged value of the conductivities of the carrier liquid and particles. In this case, the nature of the materials (carrier liquid, core, eventual shell) determines the final conductivity. In the common case of paraffin-based slurries, the thermal conductivity of the particles is lower than that of water. As a result, the thermal conductivity of the slurry is reduced, which leads to lower convective heat transfer rates.

The specific heat capacity of the slurry is the average heat capacity of the carrier liquid and particles in the so-called solid and liquid regions. To account for the latent heat of the core in the phase-changing region, an apparent heat capacity is defined. When the PCS is used as a TES fluid, the augmented heat capacity provides advantages over water, increasing the energy density. The slurry should be used primarily in this phase-changing condition, as the latent heat is involved. To consider this effect, heat transfer correlations in the phase-changing region should include the Stefan number. It has been shown by many authors that heat transfer rates are higher within this region.

The volumetric expansion coefficient is also higher in the phase-changing region due to the difference in solid and liquid densities of the core material. This results in enhanced heat transfer rates under natural convection. To define the Rayleigh number, most authors have used an averaged value of the expansion coefficient.

A summary of the effects of slurry properties on heat transfer is shown in Table 5.

CONCLUSIONS

This article presents a comprehensive review focused on the physical and heat transfer characteristics of PCSs under natural convection. PCSs are regarded as a potential enhanced fluid that can successfully replace water in low-temperature energy

Table 5. Effect of thermo-physical properties on the energy stored and heat transfer

Property	Effect on energy stored	Effect on heat transfer
Density	increases with density	increases with density
Thermal conductivity	unaffected	increases with thermal conductivity
Volumetric expansion coefficient	unaffected	increases with expansion coefficient
Specific heat capacity	increases with heat capacity	increases with specific heat capacity
Viscosity	unaffected	decreases with viscosity

storage. A thorough understanding and quantification of thermo-physical properties of natural convection of PCS is paramount for designing TES with high energy storage capacity and adequate heat transfer performance. Therefore, current knowledge and relevant gaps on this topic have been carefully reviewed.

The available models describing the physical properties of these complex fluids are critically discussed, along with providing descriptions and hints on measurement methods. We have covered density, apparent specific heat, volumetric expansion coefficient, viscosity, and thermal conductivity, together with subcooling, hysteresis, and stability effects. The volumetric expansion coefficient is often overlooked in other surveys but holds great significance in natural convection. Another fundamental aspect for natural convection heat transfer is the rheology of the fluid, which is in-depth analyzed for the dependence of viscosity on particle concentration and size, shear rate, and temperature. Overall, to the best of the authors' knowledge, this review emerges as the most comprehensive available compendium on PCS physical properties.

As for natural convection heat transfer in PCSs, it has been reviewed and grouped with respect to the geometrical configuration. The number of studies with experimental and numerical data is still limited. Moreover, numerical works are only partially validated by experiments. According to the listed works, the main findings can be summarized.

(1) Several factors contribute to the convective heat transfer: the PCS lower thermal conductivity and higher viscosity suppress convective motions, while the higher apparent specific heat and volumetric expansion coefficient promote convection.
(2) In general, heat transfer coefficient decreases with particles mass concentration.
(3) In the PCM solid and liquid region, the Nusselt number and the heat transfer coefficients are lower than in the pure carrier fluid.
(4) In the PCM phase changing region, a Nusselt number enhancement has been measured by several authors; despite the higher *Nu*, the heat transfer coefficients are typically lower, due to the lower thermal conductivity.
(5) A notable exception occurs when the PCM phase change region is near 4°C and the carrier fluid is water (a potentially common configuration in cooling applications): since water has a maximum density at 4°C, the heat transfer coefficients of the PCS are up to five times higher than those of pure water. For applications dealing with such temperatures, the convective heat transfer of the PCS is improved.
(6) Few attempts have been made to find correlations for the Nusselt number that include the phase change process, nor have classical correlations been systematically verified.

(7) The presence of subcooling and enthalpy hysteresis could increase the complexity of the model.

While the general trends in the natural convection heat transfer performance of the PCS have been identified, additional research is needed for a more comprehensive understanding and quantification of the process. Some possible research gaps and directions have been identified and are presented below.

(1) Comprehensive studies on the effect of particle size distribution on the viscosity, stability, and convection are lacking.
(2) Only few attempts have been made to establish correlations for given geometries; such correlations may be important for modeling heat exchangers for energy storage applications and for evaluating the impact of a PCS as a storage medium in a complex thermal system.
(3) Little attention has been paid to the effects of subcooling; future studies should better focus on both heating and cooling processes.
(4) Mixed convection due to weakly forced motion of the fluid bulk can play an important role in integrated TES systems. Nonetheless, to date, no studies on mixed convection have been reported.

In conclusion, further research is required to better understand and quantify the heat transfer performance of these complex fluids under natural convection, which is paramount in defining the appropriate suspension concentration to maintain acceptable heat transfer characteristics while enhancing heat storage density. In this regard, based on heat capacity calculations, a 40%–50% increase in stored energy density compared with water is expected.

Based on the characteristics of PCS outlined above, they emerge as highly promising fluids for low-temperature storage applications, with potential in various contexts, including electronic cooling, heat exchangers, solar collectors, and energy waste heat recovery. However, it is crucial to address the knowledge gaps highlighted in the review to properly engineer the PCS, design the thermal storage, and integrate it into future hybrid energy systems.

ACKNOWLEDGMENTS

This work was carried out in the framework of project NEST—Network 4 Energy Sustainable Transition—funded under the National Recovery and Resilience Plan (NRRP), Mission 4 Component 2 Investment 1.3—call for tender no. 341 of 15.03.2022 of the Italian Ministry of University and Research funded by the European UnionNextGenerationEU. The authors appreciate the cooperation of Encapsys, LLC, for kindly providing micro-encapsulated phase change material samples. The authors gratefully thank Irene Anguillesi and Davide Della Vista for fruitful discussions on measurement techniques.

AUTHOR CONTRIBUTIONS

Conceptualization, A.I.G. and D.T.; formal analysis, A.I.G. and D.R.; investigation, A.I.G. and D.R.; resources, A.I.G. and D.R.; writing – original draft, A.I.G. and D.R.; writing – review & editing, M.S. and D.T.; supervision, M.S. and D.T.; project administration, D.T.; funding acquisition, D.T.

DECLARATION OF INTERESTS

The authors declare no competing interests.

REFERENCES

1. Ritchie, H., Rosado, P., and Roser, M. (2020). Energy Production and Consumption. Our World in Data (online resource).
2. Gur, I., Sawyer, K., and Prasher, R. (2012). Searching for a Better Thermal Battery. Science (1979) *335*, 1454–1455. https://doi.org/10.1126/science.1218761.
3. The European Green Deal (2019). (European Commission).
4. Sarbu, I., and Sebarchievici, C. (2017). Introduction. In Solar Heating and Cooling Systems (Elsevier), pp. 1–11. https://doi.org/10.1016/B978-0-12-811662-3.00001-3.
5. Airò Farulla, G., Cellura, M., Guarino, F., and Ferraro, M. (2020). A Review of Thermochemical Energy Storage Systems for Power Grid Support. Appl. Sci. *10*, 3142. https://doi.org/10.3390/app10093142.
6. Abdeali, G., and Bahramian, A.R. (2022). A comprehensive review on rheological behavior of phase change materials fluids (slurry and emulsion): The way toward energy efficiency. J. Energy Storage *55*, 105549. https://doi.org/10.1016/j.est.2022.105549.
7. Mehling, H., and Cabeza, L.F. (2008). Heat and Cold Storage with PCM (Springer Berlin Heidelberg). https://doi.org/10.1007/978-3-540-68557-9.
8. Inaba, H. (2000). New challenge in advanced thermal energy transportation using functionally thermal fluids. Int. J. Therm. Sci. *39*, 991–1003. https://doi.org/10.1016/S1290-0729(00)01191-1.
9. Delgado, M., Lázaro, A., Mazo, J., and Zalba, B. (2012). Review on phase change material emulsions and microencapsulated phase change material slurries: Materials, heat transfer studies and applications. Renew. Sustain. Energy Rev. *16*, 253–273. https://doi.org/10.1016/j.rser.2011.07.152.
10. Yang, L., Liu, S., and Zheng, H. (2019). A comprehensive review of hydrodynamic mechanisms and heat transfer characteristics for microencapsulated phase change slurry (MPCS) in circular tube. Renew. Sustain. Energy Rev. *114*, 109312. https://doi.org/10.1016/j.rser.2019.109312.
11. Syah, R., Davarpanah, A., Elveny, M., and Ramdan, D. (2022). Natural convection of water and nano-emulsion phase change material inside a square enclosure to cool the electronic components. Int. J. Energy Res. *46*, 2403–2417. https://doi.org/10.1002/er.7316.
12. Kawaguchi, T., Sakai, H., Sheng, N., Kurniawan, A., and Nomura, T. (2020). Microencapsulation of Zn-Al alloy as a new phase change material for middle-high-temperature thermal energy storage applications. Appl. Energy *276*, 115487. https://doi.org/10.1016/j.apenergy.2020.115487.
13. Chen, L., You, Z., Xia, H., Tang, Q., Zhou, Y., Yao, Q., and Chen, K. (2014). Characterization of thermal and hydrodynamic properties for microencapsulated phase change slurry (MPCS). Energy Convers. Manag. *69*, 317–324. https://doi.org/10.1016/j.enconman.2013.12.026.
14. Jurkowska, M., and Szczygieł, I. (2016). Review on properties of microencapsulated phase change materials slurries (mPCMS). Appl. Therm. Eng. *98*, 365–373. https://doi.org/10.1016/j.applthermaleng.2015.12.051.
15. Kauffeld, M., and Gund, S. (2019). Ice slurry – History, current technologies and future developments. Int. J. Refrig. *99*, 264–271. https://doi.org/10.1016/j.ijrefrig.2019.01.010.
16. Albdour, S.A., Haddad, Z., Sharaf, O.Z., Alazzam, A., and Abu-Nada, E. (2022). Micro/nano-encapsulated phase-change materials (ePCMs) for solar photothermal absorption and storage: Fundamentals, recent advances, and future directions. Prog. Energy Combust. Sci. *93*, 101037. https://doi.org/10.1016/j.pecs.2022.101037.
17. Zhang, P., Ma, Z.W., and Wang, R.Z. (2010). An overview of phase change material slurries: MPCS and CHS. Renew. Sustain. Energy Rev. *14*, 598–614. https://doi.org/10.1016/j.rser.2009.08.015.
18. Morimoto, T., Ikeda, T., and Kumano, H. (2018). Study on natural convection characteristics of oil/water emulsions inside a rectangular vessel with vertical heating/cooling walls. Int. J. Heat Mass Transf. *127*, 616–628. https://doi.org/10.1016/j.ijheatmasstransfer.2018.07.053.
19. Giro-Paloma, J., Martínez, M., Cabeza, L.F., and Fernández, A.I. (2016). Types, methods, techniques, and applications for microencapsulated phase change materials (MPCM): A review. Renew. Sustain. Energy Rev. *53*, 1059–1075. https://doi.org/10.1016/j.rser.2015.09.040.
20. Cabeza, L.F., Castell, A., Barreneche, C., de Gracia, A., and Fernández, A. (2011). Materials used as PCM in thermal energy storage in buildings: A review. Renew. Sustain. Energy Rev. *15*, 1675–1695. https://doi.org/10.1016/j.rser.2010.11.018.
21. Lawag, R.A., and Ali, H.M. (2022). Phase change materials for thermal management and energy storage: A review. J. Energy Storage *55*, 105602. https://doi.org/10.1016/j.est.2022.105602.
22. Suppes, G.J., Goff, M.J., and Lopes, S. (2003). Latent heat characteristics of fatty acid derivatives pursuant phase change material applications. Chem. Eng. Sci. *58*, 1751–1763. https://doi.org/10.1016/S0009-2509(03)00006-X.
23. Piper, S.L., Kar, M., MacFarlane, D.R., Matuszek, K., and Pringle, J.M. (2022). Ionic liquids for renewable thermal energy storage – a perspective. Green Chem. *24*, 102–117. https://doi.org/10.1039/D1GC03420K.
24. Farid, M.M., Khudhair, A.M., Razack, S.A.K., and Al-Hallaj, S. (2004). A review on phase change energy storage: materials and applications. Energy Convers. Manag. *45*, 1597–1615. https://doi.org/10.1016/j.enconman.2003.09.015.
25. Ostrý, M., Bantová, S., and Struhala, K. (2020). Compatibility of Phase Change Materials and Metals: Experimental Evaluation Based on the Corrosion Rate. Molecules *25*, 2823. https://doi.org/10.3390/molecules25122823.
26. Noohi, Z., Nosouhian, S., Niroumand, B., and Timelli, G. (2022). Use of Low Melting Point Metals and Alloys (Tm < 420 °C) as Phase Change Materials: A Review. Metals *12*, 945. https://doi.org/10.3390/met12060945.
27. Zhang, P., Xiao, X., and Ma, Z.W. (2016). A review of the composite phase change materials: Fabrication, characterization, mathematical modeling and application to performance enhancement. Appl. Energy *165*, 472–510. https://doi.org/10.1016/j.apenergy.2015.12.043.
28. Zhu, J., Bai, L., Chen, B., and Fei, W. (2009). Thermodynamical properties of phase change materials based on ionic liquids. Chem. Eng. J. *147*, 58–62. https://doi.org/10.1016/j.cej.2008.11.016.
29. Bruno, F., Belusko, M., Liu, M., and Tay, N.H.S. (2015). Using solid-liquid phase change materials (PCMs) in thermal energy storage systems. In Advances in Thermal Energy Storage Systems (Elsevier), pp. 201–246. https://doi.org/10.1533/9781782420965.2.201.
30. Diaconu, B., Cruceru, M., and Anghelescu, L. (2022). Phase Change Materials—Applications and Systems Designs: A Literature Review. Designs (Basel) *6*, 117. https://doi.org/10.3390/designs6060117.
31. González-Roubaud, E., Pérez-Osorio, D., and Prieto, C. (2017). Review of commercial thermal energy storage in concentrated solar power plants: Steam vs. molten salts. Renew. Sustain. Energy Rev. *80*, 133–148. https://doi.org/10.1016/j.rser.2017.05.084.
32. Dumont, O., Frate, G.F., Pillai, A., Lecompte, S., De paepe, M., and Lemort, V. (2020). Carnot battery technology: A state-of-the-art review. J. Energy Storage *32*, 101756. https://doi.org/10.1016/j.est.2020.101756.
33. Dixit, P., Reddy, V.J., Parvate, S., Balwani, A., Singh, J., Maiti, T.K., Dasari, A., and Chattopadhyay, S. (2022). Salt hydrate phase change materials: Current state of art and the road ahead. J. Energy Storage *51*, 104360. https://doi.org/10.1016/j.est.2022.104360.
34. Wang, X., Li, W., Luo, Z., Wang, K., and Shah, S.P. (2022). A critical review on phase change materials (PCM) for sustainable and energy efficient building: Design, characteristic, performance and application. Energy Build. *260*, 111923. https://doi.org/10.1016/j.enbuild.2022.111923.
35. Alkan, C., and Sari, A. (2008). Fatty acid/poly(methyl methacrylate) (PMMA) blends as form-stable phase change materials for latent heat thermal energy storage. Sol. Energy *82*, 118–124. https://doi.org/10.1016/j.solener.2007.07.001.
36. Luo, S., He, Y., Zhu, L., Si, T., and Sun, Y. (2023). Comprehensive evaluation on the encapsulation performances of melamine-formaldehyde microcapsules affected by core

oils. Colloids Surf. A Physicochem. Eng. Asp. *659*, 130794. https://doi.org/10.1016/j.colsurfa.2022.130794.

37. Wang, X., Chen, Z., Xu, W., and Wang, X. (2019). Capric acid phase change microcapsules modified with graphene oxide for energy storage. J. Mater. Sci. *54*, 14834–14844. https://doi.org/10.1007/s10853-019-03954-2.

38. Peng, G., Dou, G., Hu, Y., Sun, Y., and Chen, Z. (2020). Phase Change Material (PCM) Microcapsules for Thermal Energy Storage. Adv. Polym. Technol. *2020*, 1–20. https://doi.org/10.1155/2020/9490873.

39. Bianco, N., Caliano, M., Fragnito, A., Iasiello, M., Mauro, G.M., and Mongibello, L. (2023). Thermal analysis of micro-encapsulated phase change material (MEPCM)-based units integrated into a commercial water tank for cold thermal energy storage. Energy *266*, 126479. https://doi.org/10.1016/j.energy.2022.126479.

40. Ghoghaei, M.S., Mahmoudian, A., Mohammadi, O., Shafii, M.B., Jafari Mosleh, H., Zandieh, M., and Ahmadi, M.H. (2021). A review on the applications of micro-/nano-encapsulated phase change material slurry in heat transfer and thermal storage systems. J. Therm. Anal. Calorim. *145*, 245–268. https://doi.org/10.1007/s10973-020-09697-6.

41. Ghasemi, K., Tasnim, S., and Mahmud, S. (2022). PCM, nano/microencapsulation and slurries: A review of fundamentals, categories, fabrication, numerical models and applications. Sustain. Energy Technol. Assessments *52*, 102084. https://doi.org/10.1016/j.seta.2022.102084.

42. Liu, L., Alva, G., Huang, X., and Fang, G. (2016). Preparation, heat transfer and flow properties of microencapsulated phase change materials for thermal energy storage. Renew. Sustain. Energy Rev. *66*, 399–414. https://doi.org/10.1016/j.rser.2016.08.035.

43. Chen, Z., and Fang, G. (2011). Preparation and heat transfer characteristics of microencapsulated phase change material slurry: A review. Renew. Sustain. Energy Rev. *15*, 4624–4632. https://doi.org/10.1016/j.rser.2011.07.090.

44. Ran, F., Chen, Y., Cong, R., and Fang, G. (2020). Flow and heat transfer characteristics of microencapsulated phase change slurry in thermal energy systems: A review. Renew. Sustain. Energy Rev. *134*, 110101. https://doi.org/10.1016/j.rser.2020.110101.

45. Konuklu, Y., Unal, M., and Paksoy, H.O. (2014). Microencapsulation of caprylic acid with different wall materials as phase change material for thermal energy storage. Sol. Energy Mater. Sol. Cell. *120*, 536–542. https://doi.org/10.1016/j.solmat.2013.09.035.

46. Heinz, A., and Streicher, W. (2006). Application of phase change materials and PCM-slurries for thermal energy storage. In 10th International Conference on Thermal Energy Storage. https://citeseerx.ist.psu.edu/document?repid=rep1&type=pdf&doi=b6e38496f5705cdf24dc0cdb4e8e6a43c76ea050.

47. Dutkowski, K., Kruzel, M., Zajączkowski, B., and Białko, B. (2020). The experimental investigation of mPCM slurries density at phase change temperature. Int. J. Heat Mass Transf. *159*, 120083. https://doi.org/10.1016/j.ijheatmasstransfer.2020.120083.

48. Kenisarin, M.M. (2014). Thermophysical properties of some organic phase change materials for latent heat storage. Sol. Energy *107*, 553–575. https://doi.org/10.1016/j.solener.2014.05.001.

49. Roy, S.K., and Avanic, B.L. (2001). Turbulent heat transfer with phase change material suspensions. Int. J. Heat Mass Transf. *44*, 2277–2285. https://doi.org/10.1016/S0017-9310(00)00260-X.

50. Chen, B., Wang, X., Zeng, R., Zhang, Y., Wang, X., Niu, J., Li, Y., and Di, H. (2008). An experimental study of convective heat transfer with microencapsulated phase change material suspension: Laminar flow in a circular tube under constant heat flux. Exp. Therm. Fluid Sci. *32*, 1638–1646. https://doi.org/10.1016/j.expthermflusci.2008.05.008.

51. Wang, L., Lee, A.Y.W., Wigg, J.P., Peshavariya, H., Liu, P., and Zhang, H. (2016). Experimental study on natural convective heat transfer of tube immersed in microencapsulated phase change material suspensions. Appl. Therm. Eng. *72*, 583–592. https://doi.org/10.1016/j.applthermaleng.2016.01.102.

52. Alisetti, E.L., and Roy, S.K. (2000). Forced Convection Heat Transfer to Phase Change Material Slurries in Circular Ducts. J. Thermophys. Heat Trans. *14*, 115–118. https://doi.org/10.2514/2.6499.

53. Hu, X., and Zhang, Y. (2002). Novel insight and numerical analysis of convective heat transfer enhancement with microencapsulated phase change material slurries: laminar flow in a circular tube with constant heat flux. Int. J. Heat Mass Transf. *45*, 3163–3172. https://doi.org/10.1016/S0017-9310(02)00034-0.

54. Fatahi, H., Claverie, J., and Poncet, S. (2022). Thermal Characterization of Phase Change Materials by Differential Scanning Calorimetry: A Review. Appl. Sci. *12*, 12019. https://doi.org/10.3390/app122312019.

55. Castellón, C., Günther, E., Mehling, H., Hiebler, S., and Cabeza, L.F. (2008). Determination of the enthalpy of PCM as a function of temperature using a heat-flux DSC-A study of different measurement procedures and their accuracy. Int. J. Energy Res. *32*, 1258–1265. https://doi.org/10.1002/er.1443.

56. Günther, E., Hiebler, S., Mehling, H., and Redlich, R. (2009). Enthalpy of Phase Change Materials as a Function of Temperature: Required Accuracy and Suitable Measurement Methods. Int. J. Thermophys. *30*, 1257–1269. https://doi.org/10.1007/s10765-009-0641-z.

57. Lazaro, A., Peñalosa, C., Solé, A., Diarce, G., Haussmann, T., Fois, M., Zalba, B., Gshwander, S., and Cabeza, L.F. (2013). Intercomparative tests on phase change materials characterisation with differential scanning calorimeter. Appl. Energy *109*, 415–420. https://doi.org/10.1016/j.apenergy.2012.11.045.

58. ASTM Standard E793, 2018: Standard test method for enthalpies of Fusion and Crystallization by Differential Scanning Calorimetry (2018). 10.1520/E0793-06R18.

59. Zhang, Y., Yi, J., and Yi, J. (1999). A simple method, the -history method, of determining the heat of fusion, specific heat and thermal conductivity of phase-change materials. Meas. Sci. Technol. *10*, 201–205. https://doi.org/10.1088/0957-0233/10/3/015.

60. Solé, A., Miró, L., Barreneche, C., Martorell, I., and Cabeza, L.F. (2013). Review of the T -history method to determine thermophysical properties of phase change materials (PCM). Renew. Sustain. Energy Rev. *26*, 425–436. https://doi.org/10.1016/j.rser.2013.05.066.

61. Marín, J.M., Zalba, B.N., Cabeza, L.F., and Mehling, H. (2003). Determination of enthalpy temperature curves of phase change materials with the temperature-history method: improvement to temperature dependent properties. Meas. Sci. Technol. *14*, 184–189. https://doi.org/10.1088/0957-0233/14/2/305.

62. Kravvaritis, E.D., Antonopoulos, K.A., and Tzivanidis, C. (2010). Improvements to the measurement of the thermal properties of phase change materials. Meas. Sci. Technol. *21*, 045103. https://doi.org/10.1088/0957-0233/21/4/045103.

63. Inaba, H., Zhang, Y., Horibe, A., and Haruki, N. (2007). Numerical simulation of natural convection of latent heat phase-change-material microcapsulate slurry packed in a horizontal rectangular enclosure heated from below and cooled from above. Heat Mass Tran. *43*, 459–470. https://doi.org/10.1007/s00231-006-0121-y.

64. Inaba, H., Dai, C., and Horibe, A. (2003). Natural convection heat transfer of microemulsion phase-change-material slurry in rectangular cavities heated from below and cooled from above. Int. J. Heat Mass Transf. *46*, 4427–4438. https://doi.org/10.1016/S0017-9310(03)00289-8.

65. Sabbah, R., Seyed-Yagoobi, J., and Al-Hallaj, S. (2012). Natural Convection With Micro-Encapsulated Phase Change Material. J. Heat Transfer *134*, 1–8. https://doi.org/10.1115/1.4006158.

66. McPhee, H., Soni, V., Saber, S., Zargartalebi, M., Riordon, J., Holmes, M., Toews, M., and Sinton, D. (2023). Rheological Behavior of Phase Change Slurries for Thermal Energy Applications. Langmuir *39*, 129–141. https://doi.org/10.1021/acs.langmuir.2c02279.

67. Einstein, A. (1906). Eine neue Bestimmung der Moleküldimensionen. Ann. Phys. *324*, 289–306. https://doi.org/10.1002/andp.19063240204.

68. Vand, V. (1945). Theory of Viscosity of Concentrated Suspensions. Nature *155*, 364–365. https://doi.org/10.1038/155364b0.

69. Charunyakorn, P., Sengupta, S., and Roy, S.K. (1991). Forced convection heat transfer in microencapsulated phase change material slurries: flow in circular ducts. Int. J. Heat Mass

Transf. *34*, 819–833. https://doi.org/10.1016/0017-9310(91)90128-2.

70. Mulligan, J.C., Colvin, D.P., and Bryant, Y.G. (1996). Microencapsulated phase-change material suspensions for heat transfer in spacecraft thermal systems. J. Spacecr. Rockets *33*, 278–284. https://doi.org/10.2514/3.26753.

71. Yamagishi, Y., Takeuchi, H., Pyatenko, A.T., and Kayukawa, N. (1999). Characteristics of microencapsulated PCM slurry as a heat-transfer fluid. AIChE J. *45*, 696–707. https://doi.org/10.1002/aic.690450405.

72. Wang, X., Niu, J., Li, Y., Wang, X., Chen, B., Zeng, R., Song, Q., and Zhang, Y. (2007). Flow and heat transfer behaviors of phase change material slurries in a horizontal circular tube. Int. J. Heat Mass Transf. *50*, 2480–2491. https://doi.org/10.1016/j.ijheatmasstransfer.2006.12.024.

73. Wu, W., Chow, L.C., Wang, C.M., Su, M., and Kizito, J.P. (2014). Jet impingement heat transfer using a Field's alloy nanoparticle – HFE7100 slurry. Int. J. Heat Mass Transf. *68*, 357–365. https://doi.org/10.1016/j.ijheatmasstransfer.2013.09.029.

74. Mooney, M. (1951). The viscosity of a concentrated suspension of spherical particles. J. Colloid Sci. *6*, 162–170. https://doi.org/10.1016/0095-8522(51)90036-0.

75. Krieger, I.M., and Dougherty, T.J. (1959). A Mechanism for Non-Newtonian Flow in Suspensions of Rigid Spheres. Trans. Soc. Rheol. *3*, 137–152. https://doi.org/10.1122/1.548848.

76. Mendoza, C.I., and Santamaría-Holek, I. (2009). The rheology of hard sphere suspensions at arbitrary volume fractions: An improved differential viscosity model. J. Chem. Phys. *130*, 044904. https://doi.org/10.1063/1.3063120.

77. Hsueh, C.H., and Wei, W.C.J. (2009). Analyses of effective viscosity of suspensions with deformable polydispersed spheres. J. Phys. D Appl. Phys. *42*, 075503. https://doi.org/10.1088/0022-3727/42/7/075503.

78. Faroughi, S.A., and Huber, C. (2015). A generalized equation for rheology of emulsions and suspensions of deformable particles subjected to simple shear at low Reynolds number. Rheol. Acta *54*, 85–108. https://doi.org/10.1007/s00397-014-0825-8.

79. Maciejewska, M., Gawdzik, B., and Rogulska, M. (2021). Regular Polymeric Microspheres with Highly Developed Internal Structure and Remarkable Thermal Stability. Materials *14*, 2240. https://doi.org/10.3390/ma14092240.

80. Chen, J., and Zhang, P. (2017). Preparation and characterization of nano-sized phase change emulsions as thermal energy storage and transport media. Appl. Energy *190*, 868–879. https://doi.org/10.1016/j.apenergy.2017.01.012.

81. Zhang, G.H., and Zhao, C.Y. (2011). Thermal and rheological properties of microencapsulated phase change materials. Renew. Energy *36*, 2959–2966. https://doi.org/10.1016/j.renene.2011.04.002.

82. Huang, L., and Petermann, M. (2015). An experimental study on rheological behaviors of paraffin/water phase change emulsion. Int J Heat Mass Transf *83*, 479–486. https://doi.org/10.1016/j.ijheatmasstransfer.2014.12.037.

83. Zhang, Z., Zhang, X., Luo, W., Yang, H., He, Y., Liu, Y., Zhang, X., and Peng, G. (2015). Experimental investigation on thermophysical properties of capric acid–lauric acid phase change slurries for thermal storage system. Energy *10*, 359–368. https://doi.org/10.1016/j.energy.2015.06.129.

84. Zhang, P., Ma, Z.W., Bai, Z.Y., and Ye, J. (2016). Rheological and energy transport characteristics of a phase change material slurry. Energy *106*, 63–72. https://doi.org/10.1016/j.energy.2016.03.025.

85. Cao, V.D., Salas-Bringas, C., Schüller, R.B., Szczotok, A.M., Hiorth, M., Carmona, M., Rodriguez, J.F., and Kjøniksen, A.L. (2018). Rheological and thermal properties of suspensions of microcapsules containing phase change materials. Colloid Polym. Sci. *296*, 981–988. https://doi.org/10.1007/s00396-018-4316-9.

86. Andrade, E.N.D.C. (1930). The Viscosity of Liquids. Nature *125*, 309–310. https://doi.org/10.1038/125309b0.

87. Tammann, G., and Hesse, W. (1926). Die Abhängigkeit der Viscosität von der Temperatur bie unterkühlten Flüssigkeiten. Z. Anorg. Allg. Chem. *156*, 245–257. https://doi.org/10.1002/zaac.19261560121.

88. Williams, M.L., Landel, R.F., and Ferry, J.D. (1955). The Temperature Dependence of Relaxation Mechanisms in Amorphous Polymers and Other Glass-forming Liquids. J. Am. Chem. Soc. *77*, 3701–3707. https://doi.org/10.1021/ja01619a008.

89. Dutkowski, K., and Fiuk, J.J. (2019). Experimental research of viscosity of microencapsulated PCM slurry at the phase change temperature. Int. J. Heat Mass Transf. *134*, 1209–1217. https://doi.org/10.1016/j.ijheatmasstransfer.2019.02.036.

90. Guyer, E.C., and Brownell, D.L. (1988). Handbook of Applied Thermal Design (McGraw-Hill).

91. Maxwell, J.C. (1873). A Treatise on Electricity and Magnetism (Clarendon press).

92. Dutkowski, K., and Kruzel, M. (2021). Experimental Investigation of the Apparent Thermal Conductivity of Microencapsulated Phase-Change-Material Slurry at the Phase-Transition Temperature. Materials *14*, 4124. https://doi.org/10.3390/ma14154124.

93. Hamilton, R.L., and Crosser, O.K. (1962). Thermal Conductivity of Heterogeneous Two-Component Systems. Ind. Eng. Chem. Fund. *1*, 187–191. https://doi.org/10.1021/i160003a005.

94. Jeffrey, D.J. (1973). Conduction through a random suspension of spheres. Proc. R. Soc. London A. Math. Phys. Sci. *335*, 355–367. https://doi.org/10.1098/rspa.1973.0130.

95. Felske, J.D. (2004). Effective thermal conductivity of composite spheres in a continuous medium with contact resistance. Int. J. Heat Mass Transf. *47*, 3453–3461. https://doi.org/10.1016/j.ijheatmasstransfer.2004.01.013.

96. Xue, Q., and Xu, W.-M. (2005). A model of thermal conductivity of nanofluids with interfacial shells. Mater. Chem. Phys. *90*, 298–301. https://doi.org/10.1016/j.matchemphys.2004.05.029.

97. Progelhof, R.C., Throne, J.L., and Ruetsch, R.R. (1976). Methods for predicting the thermal conductivity of composite systems: A review. Polym. Eng. Sci. *16*, 615–625. https://doi.org/10.1002/pen.760160905.

98. Vatani, A., Woodfield, P.L., and Dao, D.V. (2015). A survey of practical equations for prediction of effective thermal conductivity of spherical-particle nanofluids. J. Mol. Liq. *211*, 712–733. https://doi.org/10.1016/j.molliq.2015.07.043.

99. Sohn, C.W., and Chen, M.M. (1981). Microconvective Thermal Conductivity in Disperse Two-Phase Mixtures as Observed in a Low Velocity Couette Flow Experiment. J. Heat Transfer *103*, 47–51. https://doi.org/10.1115/1.3244428.

100. Liu, Z., Chen, Z., and Yu, F. (2019). Enhanced thermal conductivity of microencapsulated phase change materials based on graphene oxide and carbon nanotube hybrid filler. Sol. Energy Mater. Sol. Cell. *192*, 72–80. https://doi.org/10.1016/j.solmat.2018.12.014.

101. Günther, E., Huang, L., Mehling, H., and Dötsch, C. (2011). Subcooling in PCM emulsions – Part 2: Interpretation in terms of nucleation theory. Thermochim. Acta *522*, 199–204. https://doi.org/10.1016/j.tca.2011.04.027.

102. Diaconu, B.M., Varga, S., and Oliveira, A.C. (2010). Experimental assessment of heat storage properties and heat transfer characteristics of a phase change material slurry for air conditioning applications. Appl. Energy *87*, 620–628. https://doi.org/10.1016/j.apenergy.2009.05.002.

103. Bain, A. (2022). Buoyancy and Brownian motion of plastics in aqueous media: predictions and implications for density separation and aerosol internal mixing state. Environ. Sci.: Nano *9*, 4249–4254. https://doi.org/10.1039/D2EN00525E.

104. Yamagishi, Y., Sugeno, T., Ishige, T., Takeuchi, H., and Pyatenko, A.T. (1996). An evaluation of microencapsulated PCM for use in cold energy transportation medium. In IECEC 96. Proceedings of the 31st Intersociety Energy Conversion Engineering Conference (IEEE), pp. 2077–2083. https://doi.org/10.1109/IECEC.1996.553442.

105. Gschwander, S., Schossig, P., and Henning, H. (2005). Micro-encapsulated paraffin in phase-change slurries. Sol. Energy Mater. Sol. Cell. *89*, 307–315. https://doi.org/10.1016/j.solmat.2004.12.008.

106. Kong, M., Alvarado, J.L., Thies, C., Morefield, S., and Marsh, C.P. (2017). Field evaluation of microencapsulated phase change material slurry in ground source heat pump systems. Energy *122*, 691–700. https://doi.org/10.1016/j.energy.2016.12.092.

107. Bejan, A. (2013). Convection Heat Transfer (Wiley). https://doi.org/10.1002/9781118671627.

108. Ayuob, S., Mahmood, M., Ahmad, N., Waqas, A., Saeed, H., and Sajid, M.B. (2022). Development and validation of Nusselt number correlations for a helical coil based energy storage integrated with solar water heating system. J. Energy Storage *55*, 105777. https://doi.org/10.1016/j.est.2022.105777.

109. Inaba, H., Dai, C., and Horibe, A. (2003). Numerical simulation of Rayleigh–Bénard convection in non-Newtonian phase-change-material slurries. Int. J. Therm. Sci. *42*, 471–480. https://doi.org/10.1016/S1290-0729(02)00048-0.

110. Delgado, M., Lázaro, A., Mazo, J., Peñalosa, C., Dolado, P., and Zalba, B. (2015). Experimental analysis of a low cost phase change material emulsion for its use as thermal storage system. Energy Convers. Manag. *106*, 201–212. https://doi.org/10.1016/j.enconman.2015.09.033.

111. Morimoto, T., and Kumano, H. (2022). Natural convection characteristics of phase-change material emulsions in a rectangular vessel with vertical heating/cooling walls. Int. J. Heat Mass Transf. *183*, 122234. https://doi.org/10.1016/j.ijheatmasstransfer.2021.122234.

112. Diaconu, B.M., Varga, S., and Oliveira, A.C. (2010). Experimental study of natural convection heat transfer in a microencapsulated phase change material slurry. Energy *35*, 2688–2693. https://doi.org/10.1016/j.energy.2009.06.028.

113. Huang, M.J., Eames, P.C., McCormack, S., Griffiths, P., and Hewitt, N.J. (2011). Microencapsulated phase change slurries for thermal energy storage in a residential solar energy system. Renew. Energy *36*, 2932–2939. https://doi.org/10.1016/j.renene.2011.04.004.

114. Zhang, Y., Wang, S., Rao, Z., and Xie, J. (2011). Experiment on heat storage characteristic of microencapsulated phase change material slurry. Sol. Energy Mater. Sol. Cell. *95*, 2726–2733. https://doi.org/10.1016/j.solmat.2011.02.015.

115. Zhang, Y., Rao, Z., Wang, S., Zhang, Z., and Li, X. (2012). Experimental evaluation on natural convection heat transfer of microencapsulated phase change materials slurry in a rectangular heat storage tank. Energy Convers. Manag. *59*, 33–39. https://doi.org/10.1016/j.enconman.2012.02.004.

116. Li, W., Wan, H., Zhang, P., Liu, P., He, G., and Qin, F. (2018). A method to evaluate natural convection heat transfer in microencapsulated phase change material (MPCM) slurry: An experimental study. Int. Commun. Heat Mass Tran. *96*, 1–6. https://doi.org/10.1016/j.icheatmasstransfer.2018.05.011.

117. Allouche, Y., Varga, S., Bouden, C., and Oliveira, A.C. (2015). Experimental determination of the heat transfer and cold storage characteristics of a microencapsulated phase change material in a horizontal tank. Energy Convers. Manag. *94*, 275–285. https://doi.org/10.1016/j.enconman.2015.01.064.

118. Allouche, Y., Varga, S., Bouden, C., and Oliveira, A.C. (2016). Validation of a CFD model for the simulation of heat transfer in a tubes-in-tank PCM storage unit. Renew. Energy *89*, 371–379. https://doi.org/10.1016/j.renene.2015.12.038.

119. Ghalambaz, M., Chamkha, A.J., and Wen, D. (2019). Natural convective flow and heat transfer of Nano-Encapsulated Phase Change Materials (NEPCMs) in a cavity. Int. J. Heat Mass Transf. *138*, 738–749. https://doi.org/10.1016/j.ijheatmasstransfer.2019.04.037.

120. Hajjar, A., Mehryan, S.A.M., and Ghalambaz, M. (2020). Time periodic natural convection heat transfer in a nano-encapsulated phase-change suspension. Int. J. Mech. Sci. *166*, 105243. https://doi.org/10.1016/j.ijmecsci.2019.105243.

121. Ghalambaz, M., Jin, H., Bagheri, A., Younis, O., and Wen, D. (2022). Convective Flow and Heat Transfer of Nano-Encapsulated Phase Change Material (Nepcm) Dispersions Along a Vertical Surface. FU. Mech. Eng. *20*, 519–538. https://doi.org/10.22190/FUME220603034G.

122. Saramito, P. (2016). Complex Fluids Modeling and Algorithms (Springer International Publishing).

123. Ozoe, H., and Churchill, S.W. (1972). Hydrodynamic stability and natural convection in Ostwald-de Waele and Ellis fluids: The development of a numerical solution. AIChE J. *18*, 1196–1207. https://doi.org/10.1002/aic.690180617.

124. Globe, S., and Dropkin, D. (1959). Natural-Convection Heat Transfer in Liquids Confined by Two Horizontal Plates and Heated From Below. J. Heat Transfer *81*, 24–28. https://doi.org/10.1115/1.4008124.

125. Bai, Z., Miao, Y., Xu, H., and Gao, Q. (2020). Experimental study on thermal storage and heat transfer performance of microencapsulated phase-change material slurry. Therm. Sci. Eng. Prog. *17*, 100362. https://doi.org/10.1016/j.tsep.2019.100362.